Impurities and graphene hybrid structures: insights from first-principles theory

Tim Wehling

Institute for Theoretical Physics
and
Bremen Center for Computational Materials Science

University of Bremen

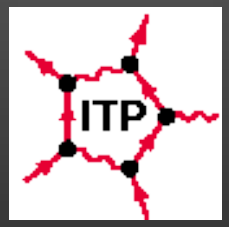

Collaborations

U. Hamburg

B. Sachs, M. Karolak, A. Lichtenstein

U. Nijmegen

S. Yuan, M. Katsnelson

U. Cologne

A. Rosch

LANL

A. Balatsky

U. Cologne

D. Förster, S. Schumacher, C. Busse, T. Michely

U. Kiel

S. Altenburg, R. Berndt

TU Ilmenau

J. Kröger

U. Hamburg

M. Gyamfi, M. Wasniowska, R. Wiesendanger

Outline

- Defects in graphene
  - Covalent adsorbates versus vacancies
  - Transition metal adatoms
- Graphene hybrid structures
  - Graphene on metals
  - Interaction of graphene with hBN substrates

Local impurities in “Dirac materials”

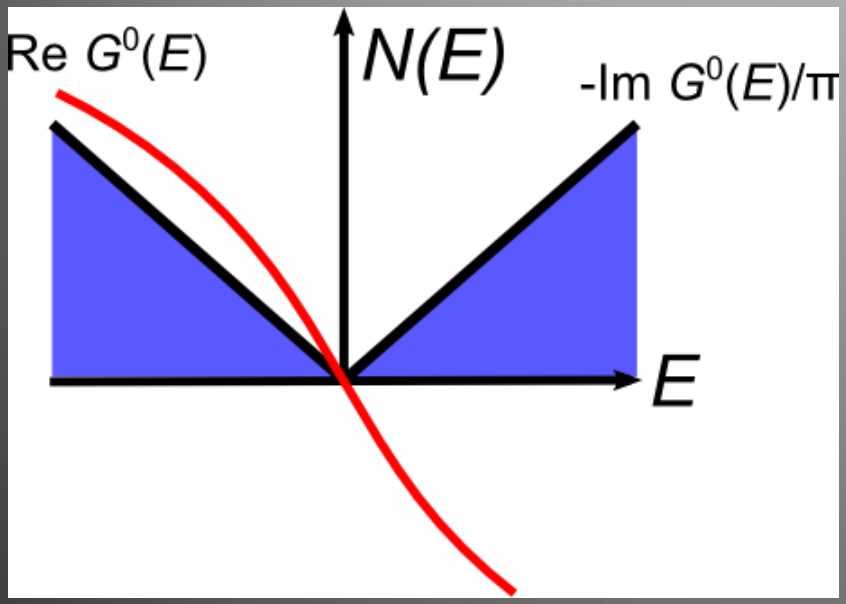

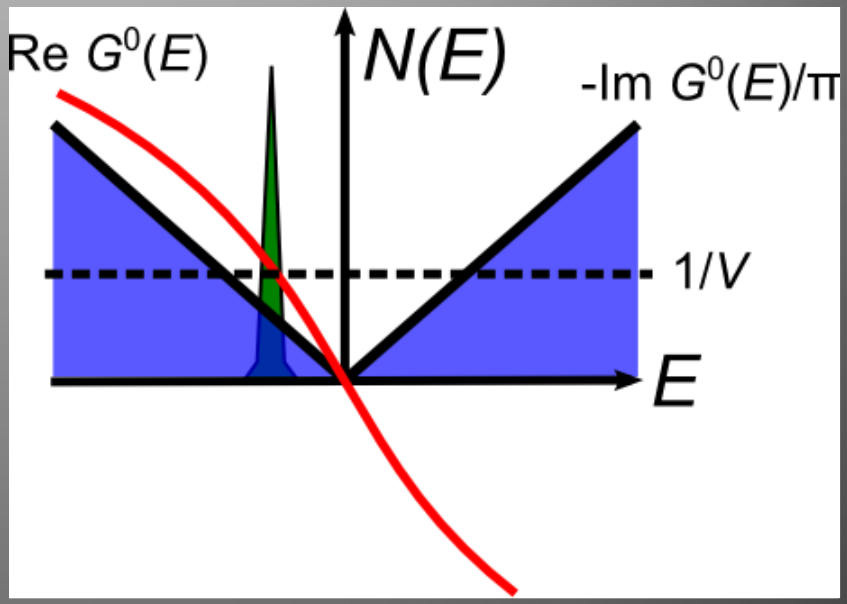

Point defect:

δ-function potential

$$V(x) = V\delta(x)$$
$$\hat{V} = V\sum_{k,k'} c_k^\dagger c_{k'}$$

Green‘s functions and T-matrix

$$\hat{G}(E) = \hat{G}^0(E) + \hat{G}^0(E)\hat{T}(E)\hat{G}^0(E)$$
$$\hat{T}(E) = \left(\mathbf{1} - \hat{V}\hat{G}^0(E)\right)^{-1}\hat{V}$$

Balatsky, Vekther, Zhu, RMP (2006)

Tight binding model of localized impurities in graphene

- Pristine material

$$\hat{H} = t \sum_{<i,j>} a_i^\dagger b_j + a_j^\dagger b_i$$

- Impurity potentials

$$\hat{V} = \sum_{i,j} \Psi_i^\dagger V_{i,j} \Psi_j;\ \Psi_i = (a_i, b_i)$$

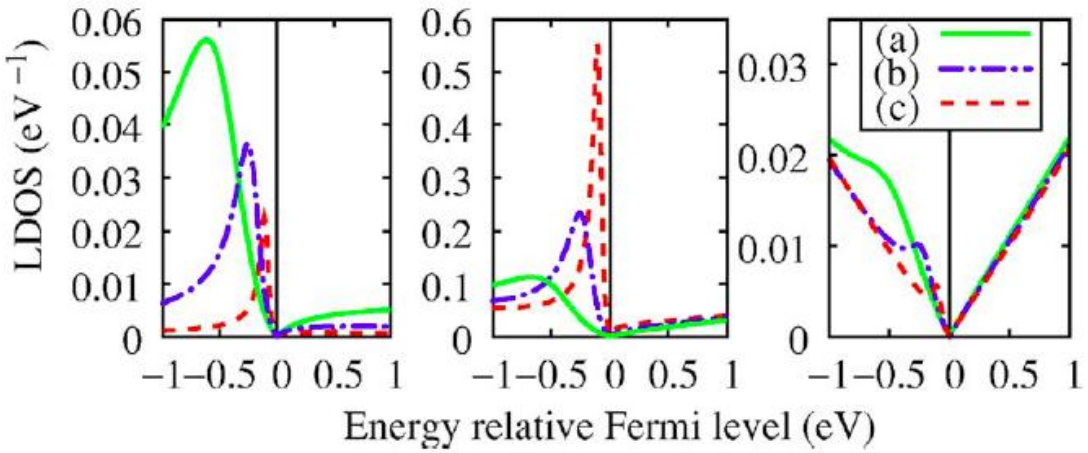

FIG. 3. (Color online) LDOSs at the impurity site (left), NN site (middle), and NNN site (right) are shown for a single impurity with potentials U_0=(a) 10 eV, (b) 20 eV, and (c) 40 eV.

Single site impurities

$$V_{0,0} = V_s = U_0 \begin{pmatrix} 1 & 0 \\ 0 & 0 \end{pmatrix}$$

TW et al., PRB **75**, 125425 (2007).
TW et al., CPL **476**, 125 (2009).

Vacancies in graphene

PHYSICAL REVIEW B VOLUME 17, NUMBER 2 15 JANUARY 1978

Self-consistent LCAO calculation of the electronic properties of graphite. II. Point vacancy in the two-dimensional crystal

Alex Zunger* and R. Englman

Department of Theoretical Physics and Applied Mathematics, Soreq Nuclear Research Centre, Yavne, Israel

(Received 11 August 1975)

The electronic properties of a point vacancy in the two-dimensional graphite crystal are investigated within the small-periodic-cluster approach using a self-consistent all-valence-electron LCAO (linear combination of atomic orbitals) scheme previously employed for the calculations of the band structure and optical spectra of the regular lattice (part I). Eight crystal bands, 54-96 $\vec{K}$ points in the Brillouin zone, selected according to the "mean value theorem" and 2^2-5^2 primitive unit cells around the defect site are allowed to interact. A doubly degenerate singly occupied σ defect level is shown to appear in the σ-σ^* band gap, 3.5 eV above the σ band edge, with a wave function that is about 80% localized on the three nearest-neighbor atoms. The density of

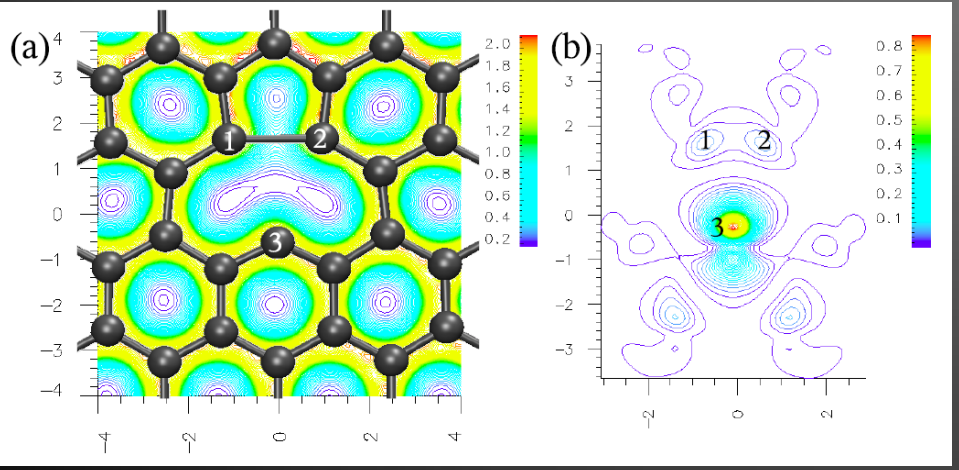

Left: Electronic density (a) and spin density (b) around a vacancy defect in graphene.

P.O. Lehtinen et al PRL (2004)

Right: Spin-polarized DOS near vacancy in graphene.

O. Yazyev and L. Helm PRB (2007)

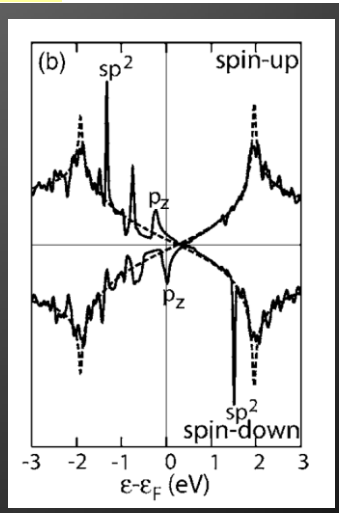

Covalently bound impurities

- Impurities with additional orbitals

$$\hat{H}_{\mathrm{imp}} = \epsilon_d d^\dagger d \qquad \hat{V} = \sum_i \Psi_i^\dagger V_i d + \mathrm{H.c.}$$

- Effective potential on host electrons

$$V_{k,k'}(E) = \frac{V_k^* V_{k'}}{E - \epsilon_d}$$

- Midgap state in graphene if:

$$|\epsilon_d| \ll D \text{ and } V_k = V \gtrsim D$$

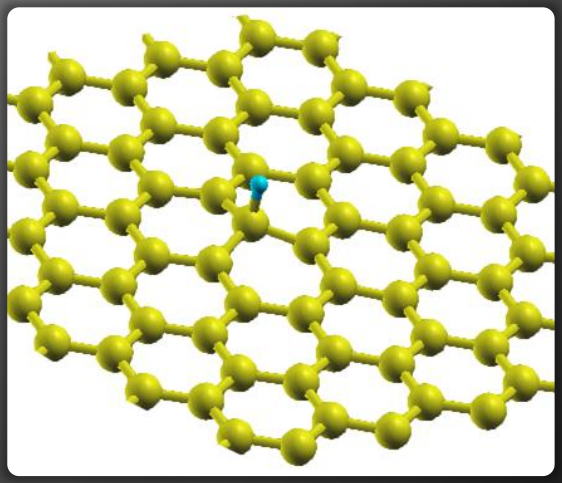

Hydrogen adatom on graphene

Realistic model of resonant impurities

Organic groups adsorbed to graphene

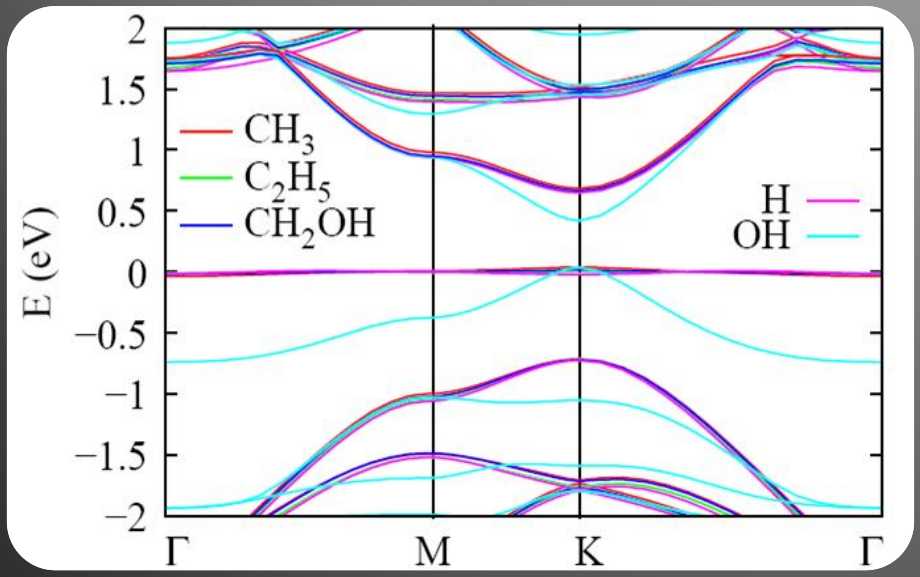

Supecell band structures from DFT

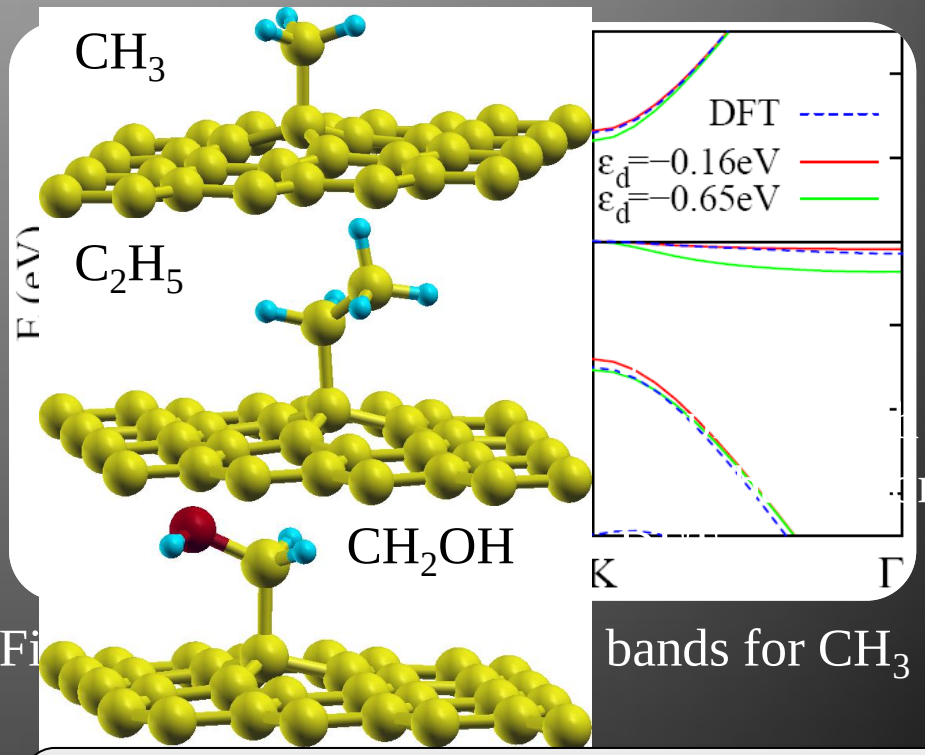

Fi bands for CH_3

C – impurity hopping: $|V| \gtrsim 2t$

Imp. on-site energy: $|\epsilon_d| \lesssim 0.1t$

Low energy resonances within ~0.03eV around Dirac point

Covalent versus ionic bonding

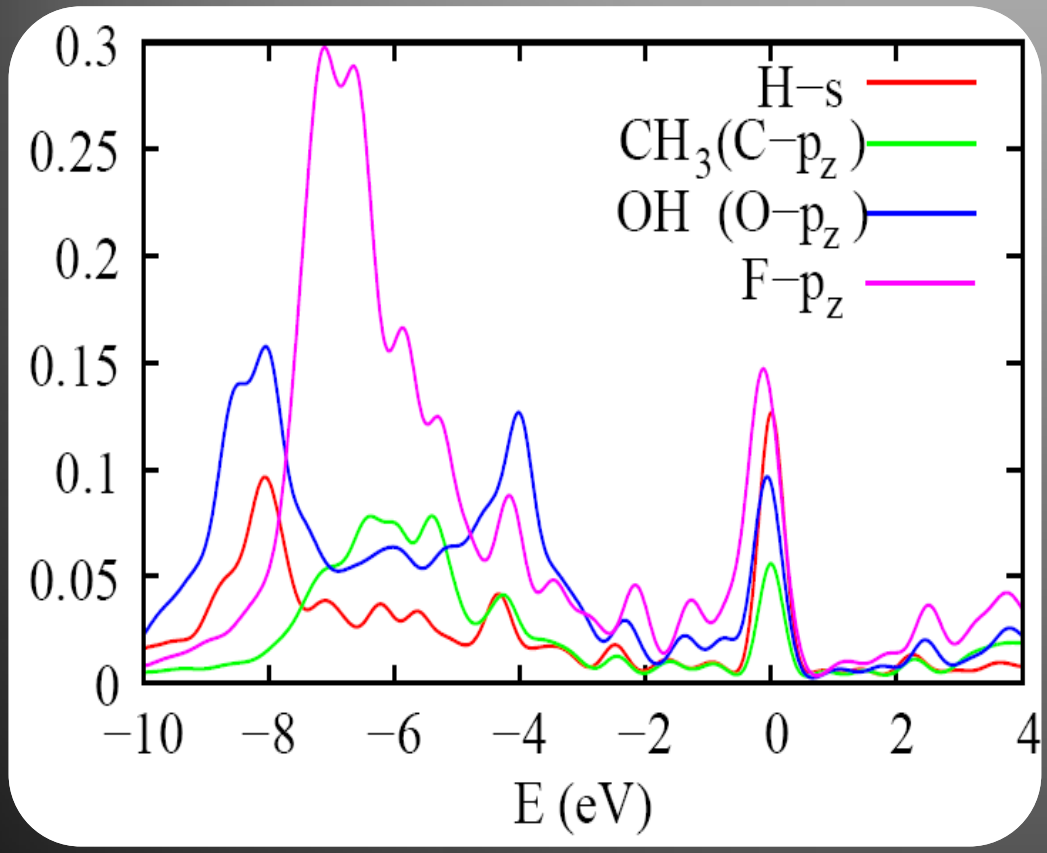

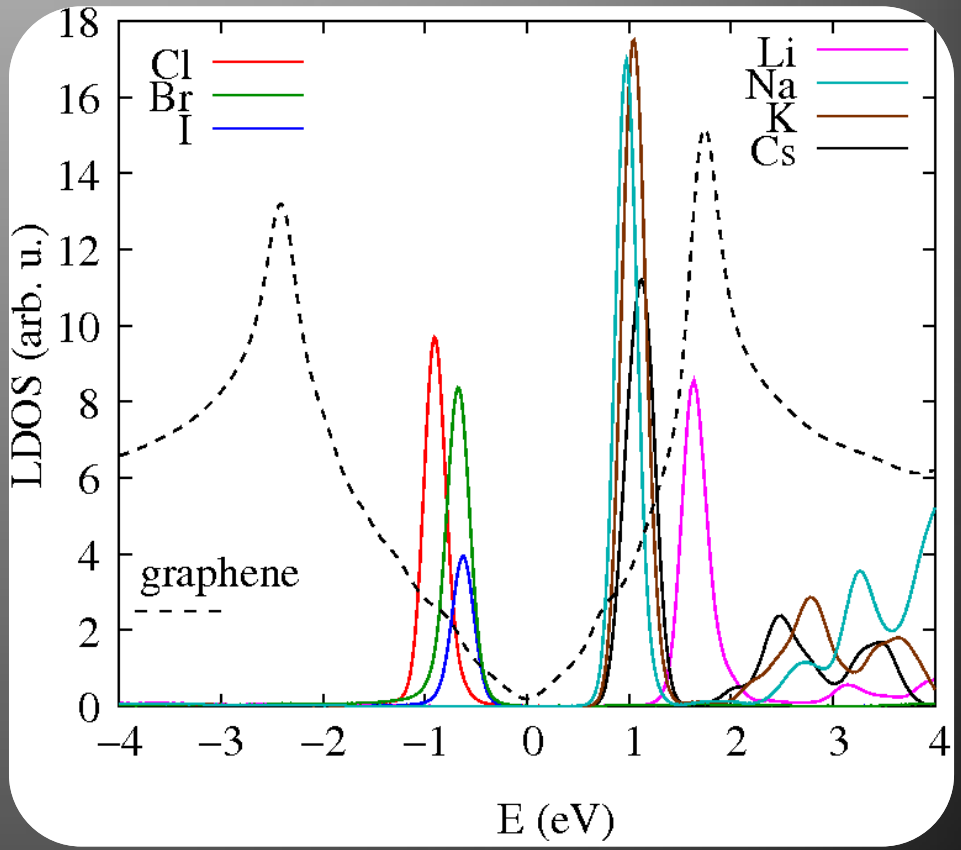

Local density of states at the impurity site

TW et al., Phys. Rev. B **80**, 085428 (2009)

INTERACTION OF TRANSITION METALS WITH GRAPHENE

Symmetry analysis

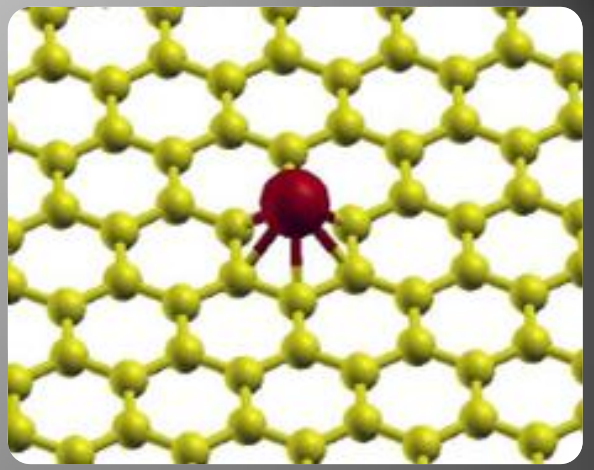

Adatoms at h-site:

- irreducible representations of C_{6v} point symmetry
  - Atomic *d*-orbitals
    $= E_1 + E_2 + A_1$
  - Graphene Dirac electrons
    $= E_1 + E_2$

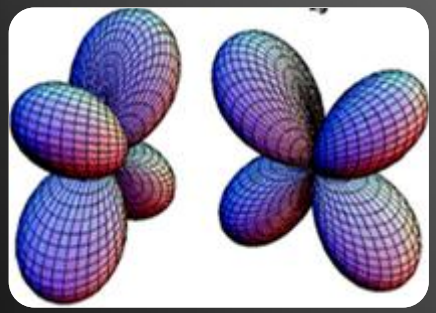

E_1 (d_{xz}, d_{yz}); $|l_z|=1$

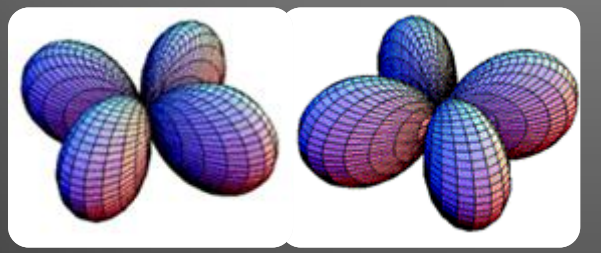

E_2 (d_{xy}, $d_{x^2-y^2}$); $|l_z|=2$

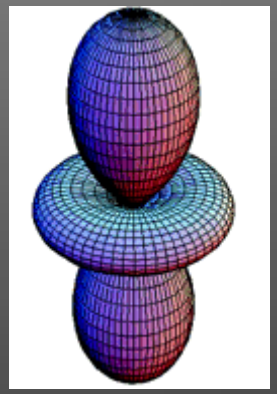

A_1 (d_{z^2}); $l_z=0$

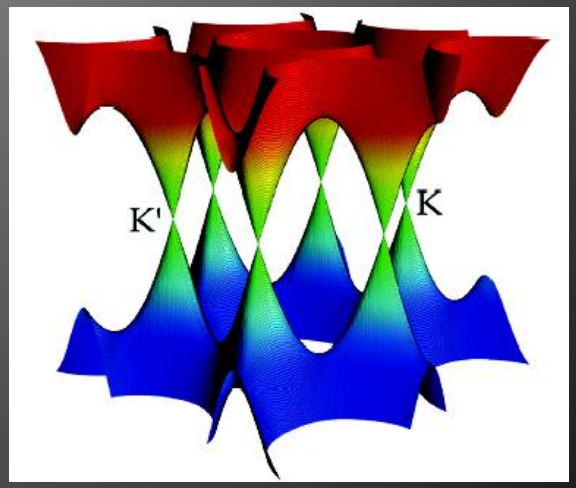

TW et al., PRB **81**, 115427 (2010)

Orbital selective coupling of Ni adatoms to graphene

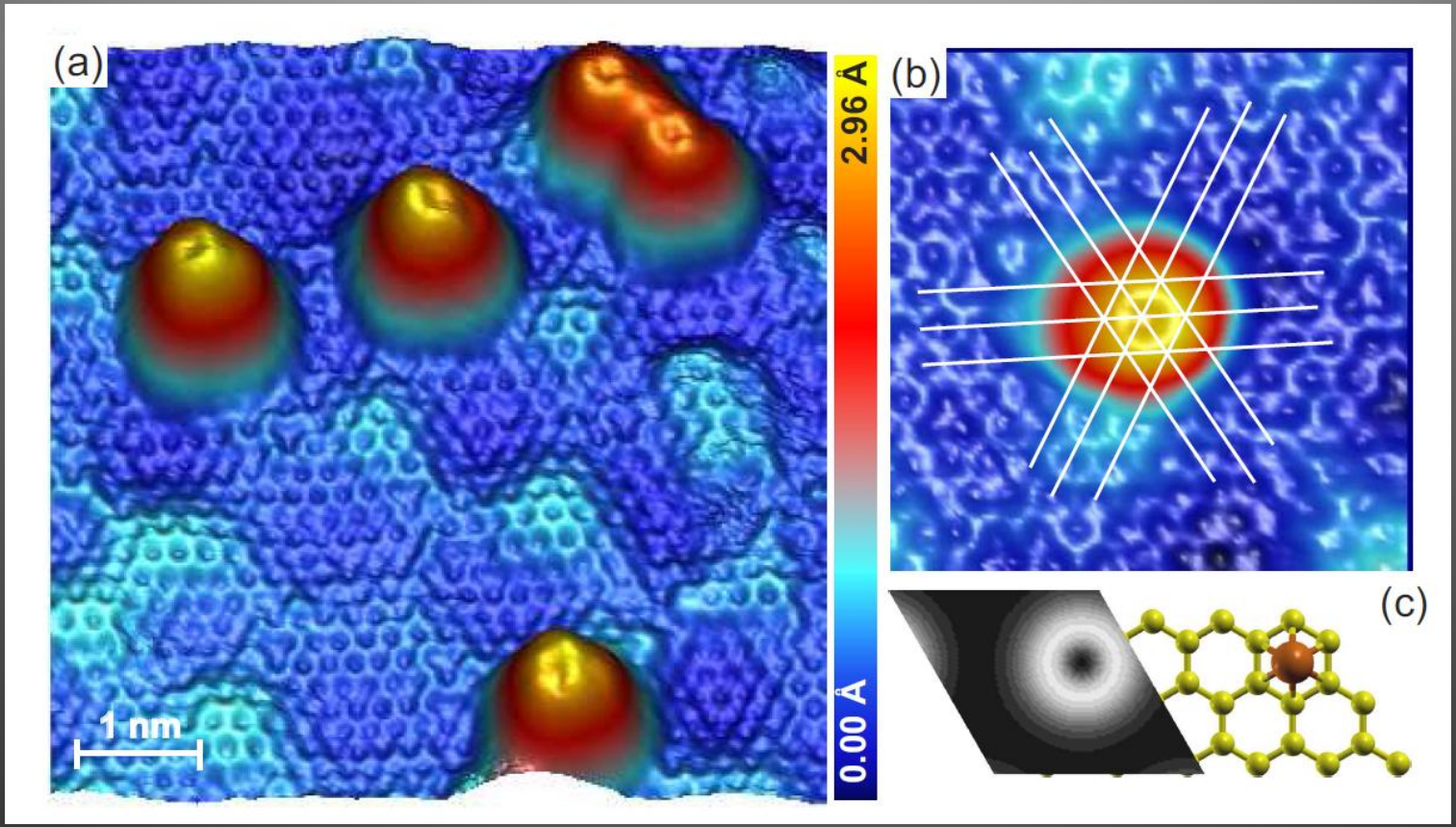

(a) Topographic image of Ni monomers on graphene. (b) STM topography indicating the adatom's position on graphene. STM experiments: Wiesendanger group (Hamburg).

(c) Simulated LDOS in the vacuum above a single Ni adatom on graphene (left) and adsorption geometry of the adatom (right).

Co adatoms on graphene

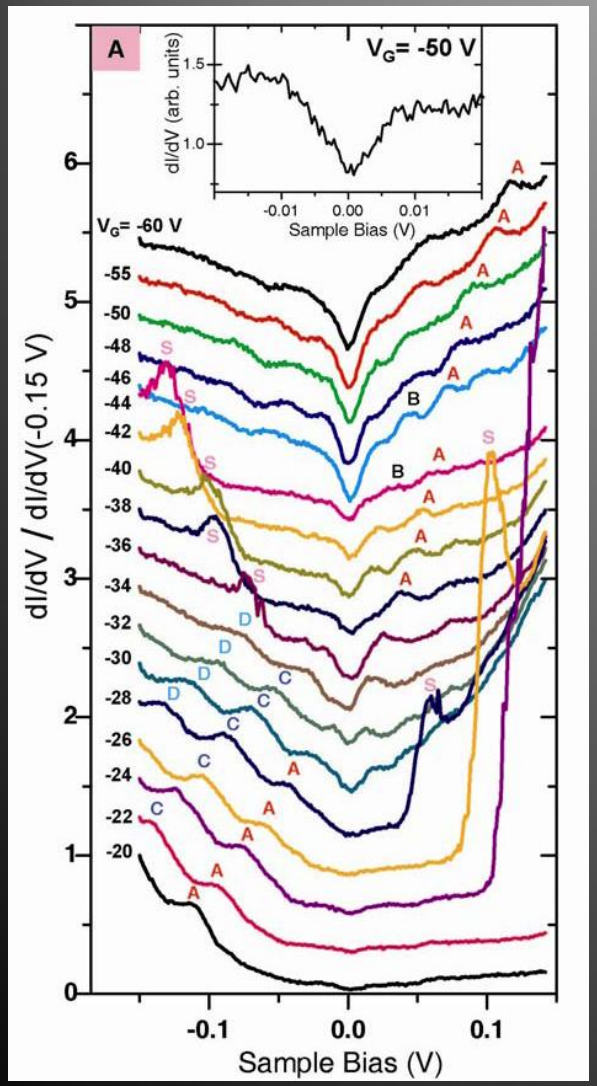

STS spectra of Co on graphene

V. Brar, Nature Phys. 7, 43 (2010)

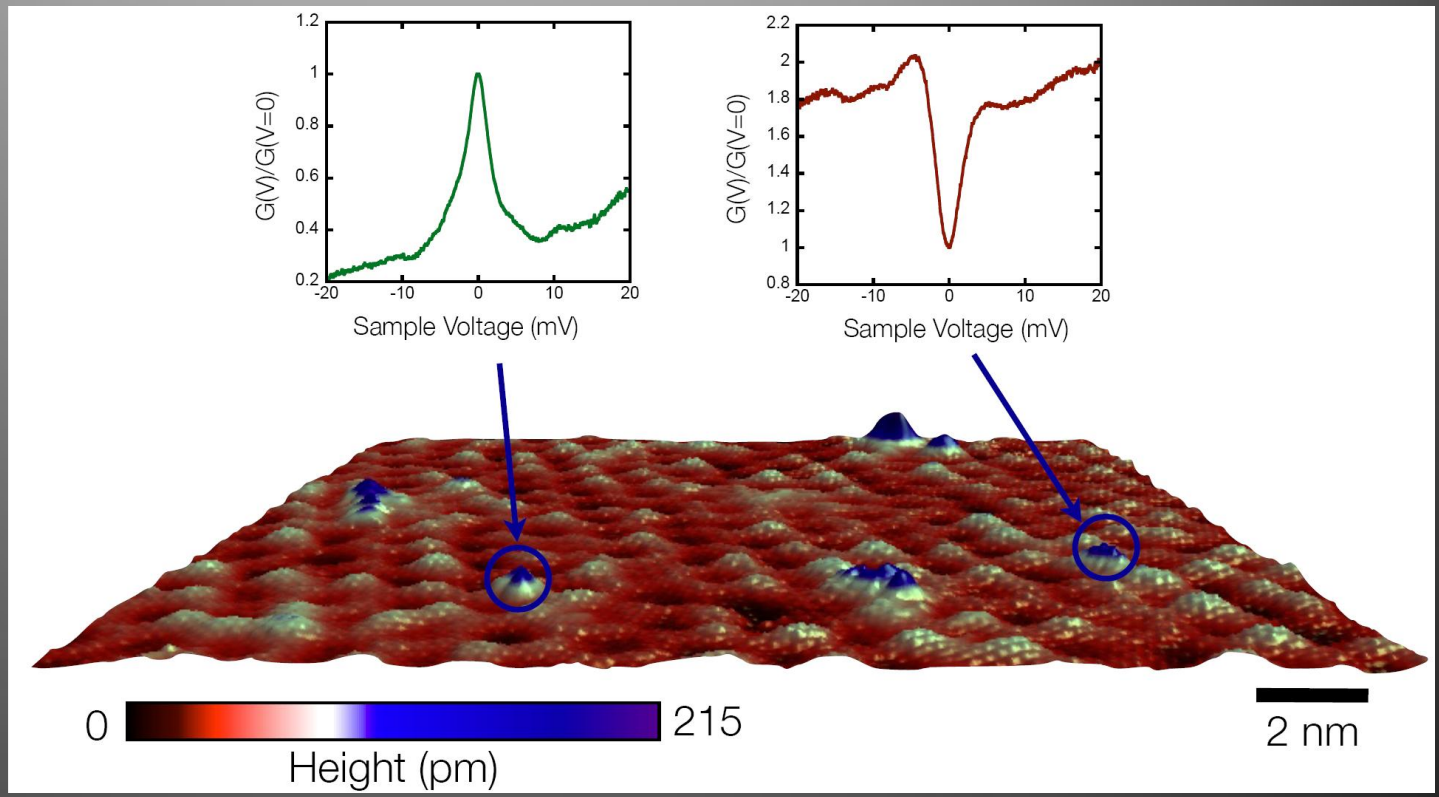

STS and topography of Co on graphene

H. Manoharan et al., Nature under review

Co on graphene at h-site: electronic structure

S=1/2

$E_1=d_{xz}, d_{yz}$

$E_2=d_{xy}, d_{x^2-y^2}$

$A_1=d_{3r^2-z^2}$

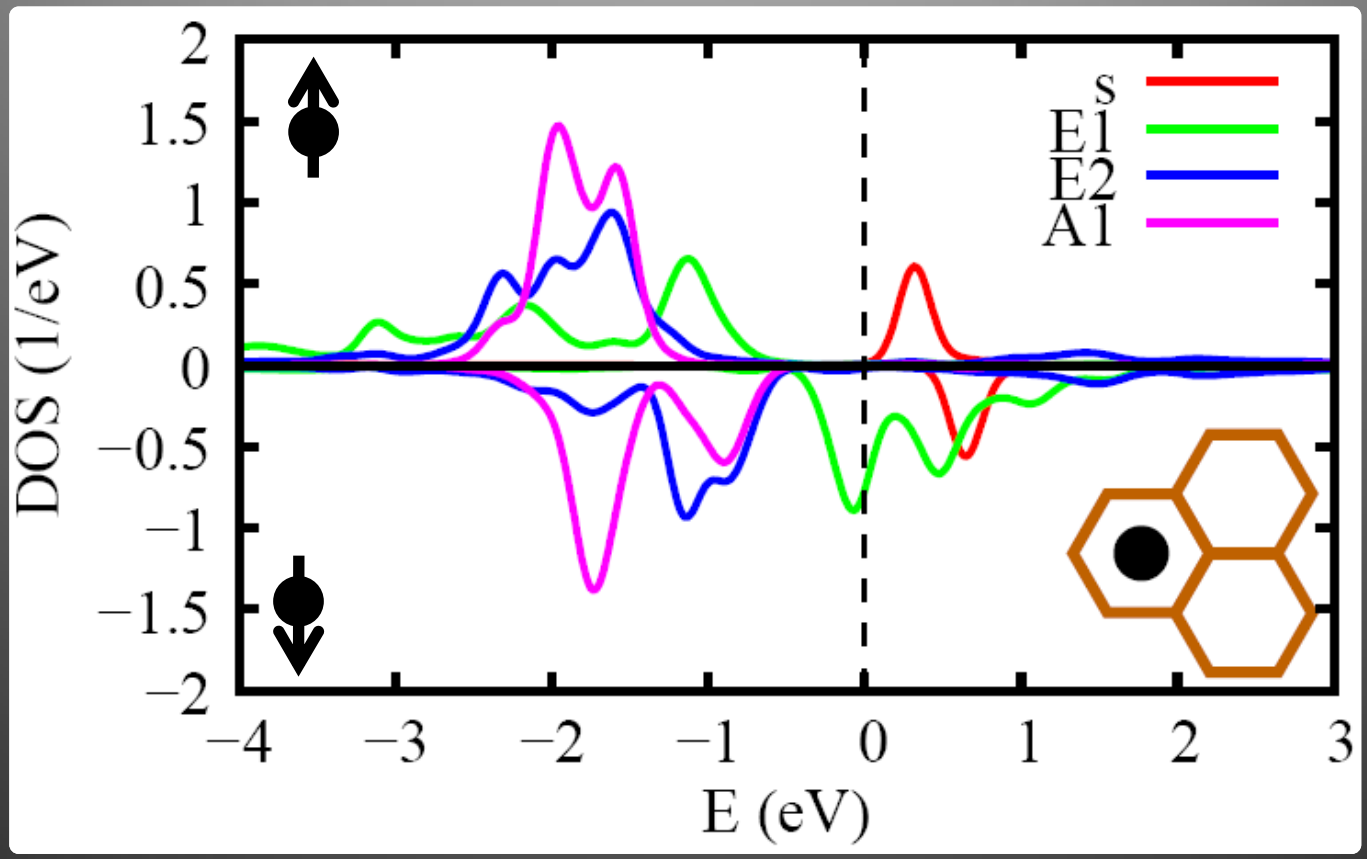

TW et al., PRB **81**, 115427 (2010)

Spin and orbital resolved density of states at Co site from GGA+U (U=2eV, J=0.9eV). Spin up positive, spin down negative ordinate.

Scenarios for Kondo effect: Co at h-site

Energy level diagram

$E_2=d_{xy}, d_{x^2-y^2}$; $E_1=d_{xz}, d_{yz}$; $A_1=d_{3r^2-z^2}$

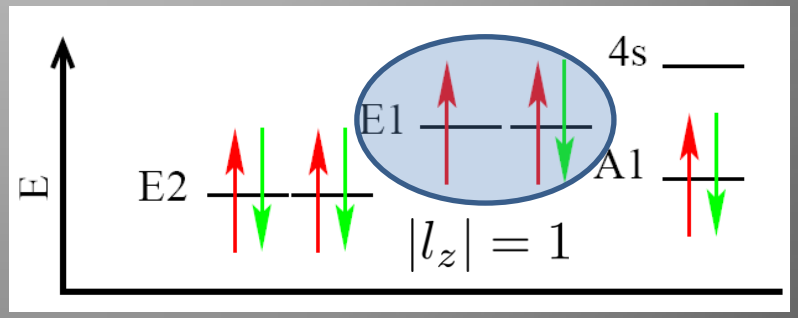

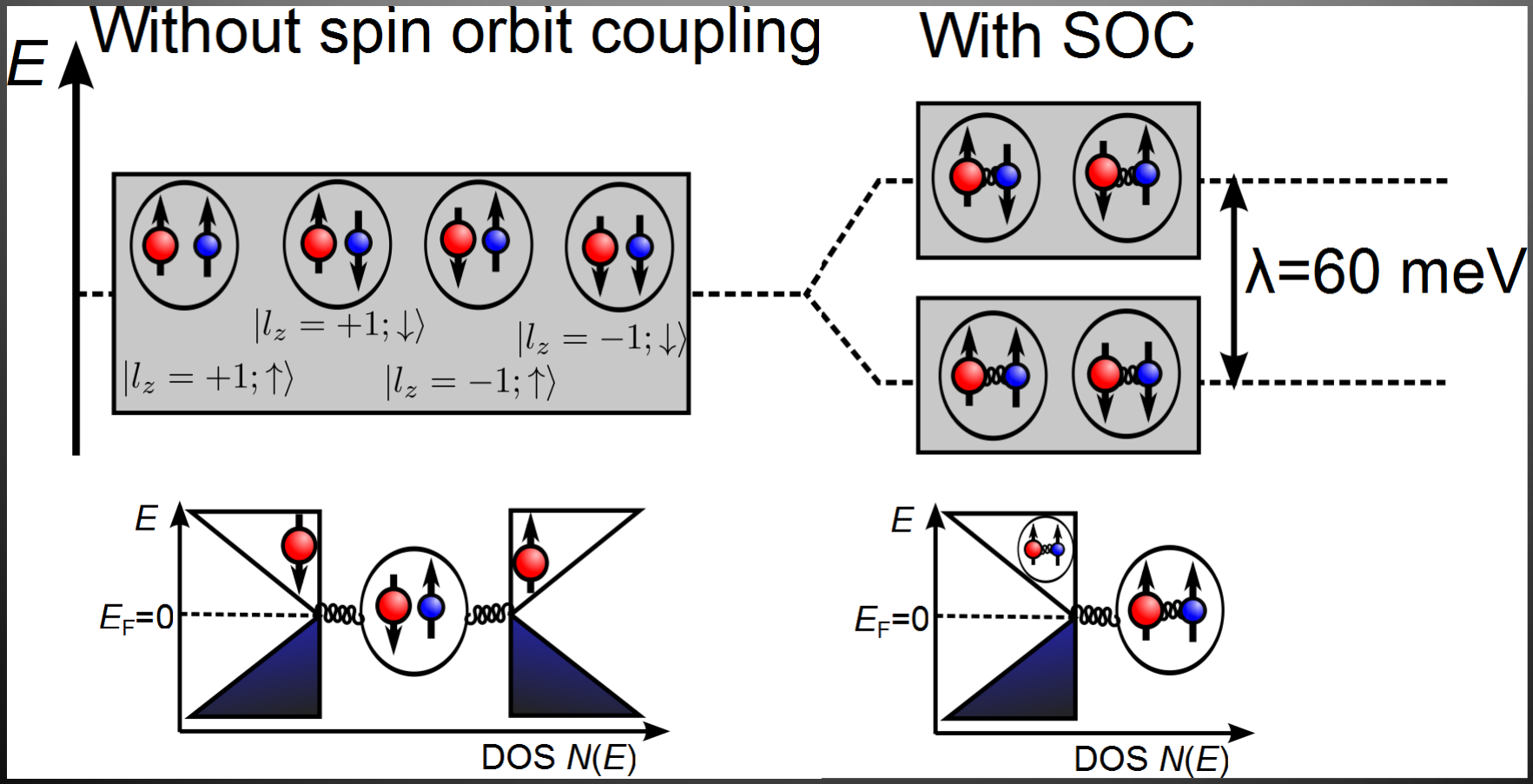

Realistic models of strongly correlated electron systems

Anderson impurity model

$$\hat{H}_{\mathrm{AIM}} = \sum_{k,\sigma} \epsilon_k c^\dagger_{k,\sigma} c_{k,\sigma} + \sum_{k,m,\sigma} \left(V_{km} c^\dagger_{k,\sigma} d_{m,\sigma} + \mathrm{H.c.} \right) + \hat{H}_{\mathrm{at}}$$

$$\hat{H}_{\mathrm{at}} = \sum_{m,\sigma} \epsilon_{d,m} d^\dagger_{m,\sigma} d_{m,\sigma} + \frac{1}{2} \sum_{\substack{m,m,'m'',m''' \\ \sigma,\sigma'}} U_{mm'm''m'''} d^\dagger_{m,\sigma} d^\dagger_{m',\sigma'} d_{m'',\sigma'} d_{m''',\sigma}$$

Hybridization function

$$\Delta_{mm'}(\omega) = \sum_k \frac{V^*_{km} V_{km'}}{\omega + i0^+ - \epsilon_k}$$

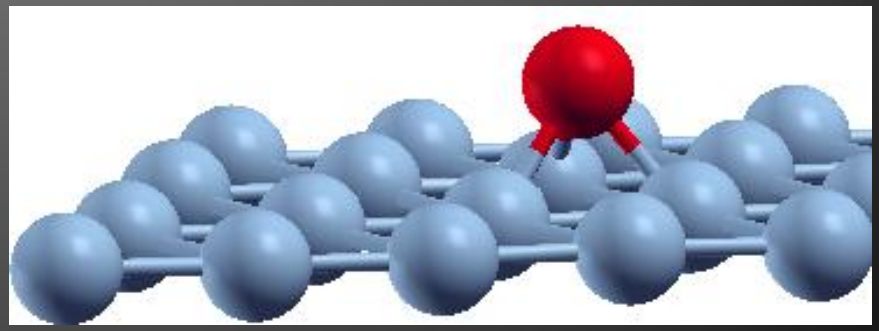

Interface of DFT to many body methods

Projector mapping

Idea: Use of projections of DFT wave functions $|K\rangle$ onto localized orbitals $|L\rangle$ to obtain hybridization functions

Local Green function and hybridization function

$$\hat{G}_0^{\mathrm{loc}}(\omega) = \sum_{K,L,L'} |L\rangle \frac{\langle L|K\rangle\langle K|L'\rangle}{\omega + i0^+ - \epsilon_K} \langle L'|$$

$$\hat{\Delta}(\omega) = \omega + i\delta - \epsilon_d - \left[\hat{G}_0^{\mathrm{loc}}(\omega)\right]^{-1}$$

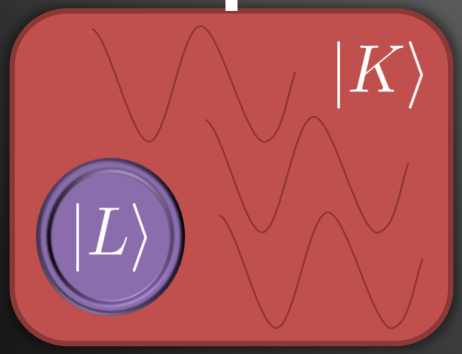

Projector augmented wave basis

$$|K\rangle = |\tilde{K}\rangle + \sum_i (|\phi_i\rangle - |\tilde{\phi}_i\rangle)\langle \tilde{p}_i|\tilde{K}\rangle$$

$$|L\rangle = |\phi_i\rangle$$

$$\langle L|K\rangle = \sum_{\nu'} \langle L|\phi_{\nu'}\rangle\langle \tilde{p}_{\nu'}|\tilde{K}\rangle$$

Implementation with VASP code

PRB **77**, 205112 (2008), PRB **81**, 085413 (2010), J. Phys.: Condens Matter 23 (2011) 085601

Co at h-site: hybridization functions

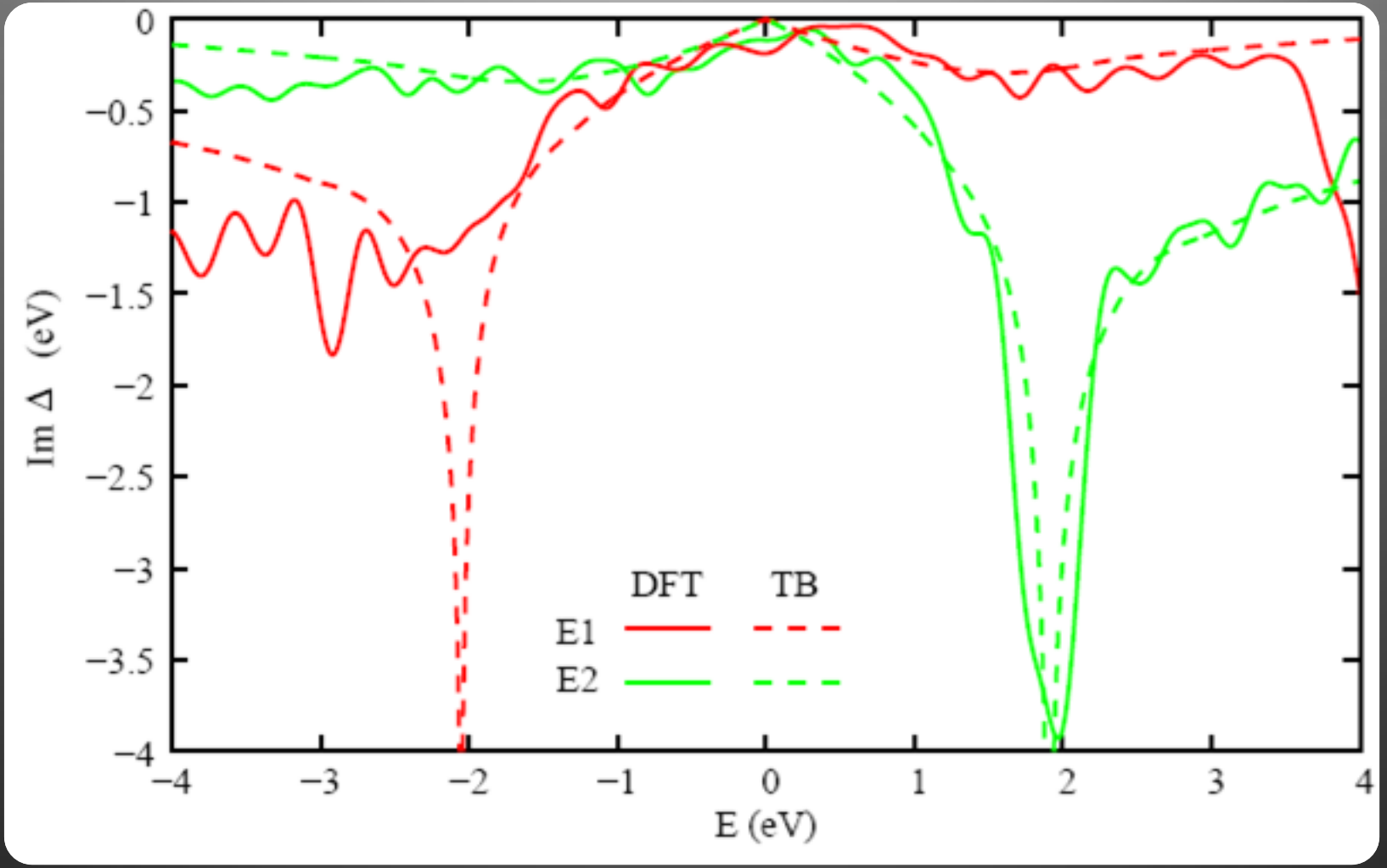

TW et al., PRB **81**, 115427 (2010)

Particle hole asymmetry of hybridization functions due to coupling to vHS

Co at h-site: Poor man‘s scaling

- RG study of Kondo effect

$$\frac{\mathrm{d}J(D)}{\mathrm{d}D} = -N(D)J^2(D)\frac{\rho(\mu - D) + \rho(\mu + D)}{2D},$$

  - effective degeneracy factor

$$N(D) = 4 \text{ for } D > \lambda \text{ and } N(D) = 2 \text{ else}$$

  - effective DOS

$$\rho(\omega) = -\frac{\mathrm{Im}\,\Delta_1(\omega)}{\pi V_1^2}$$

RG flow of effective coupling

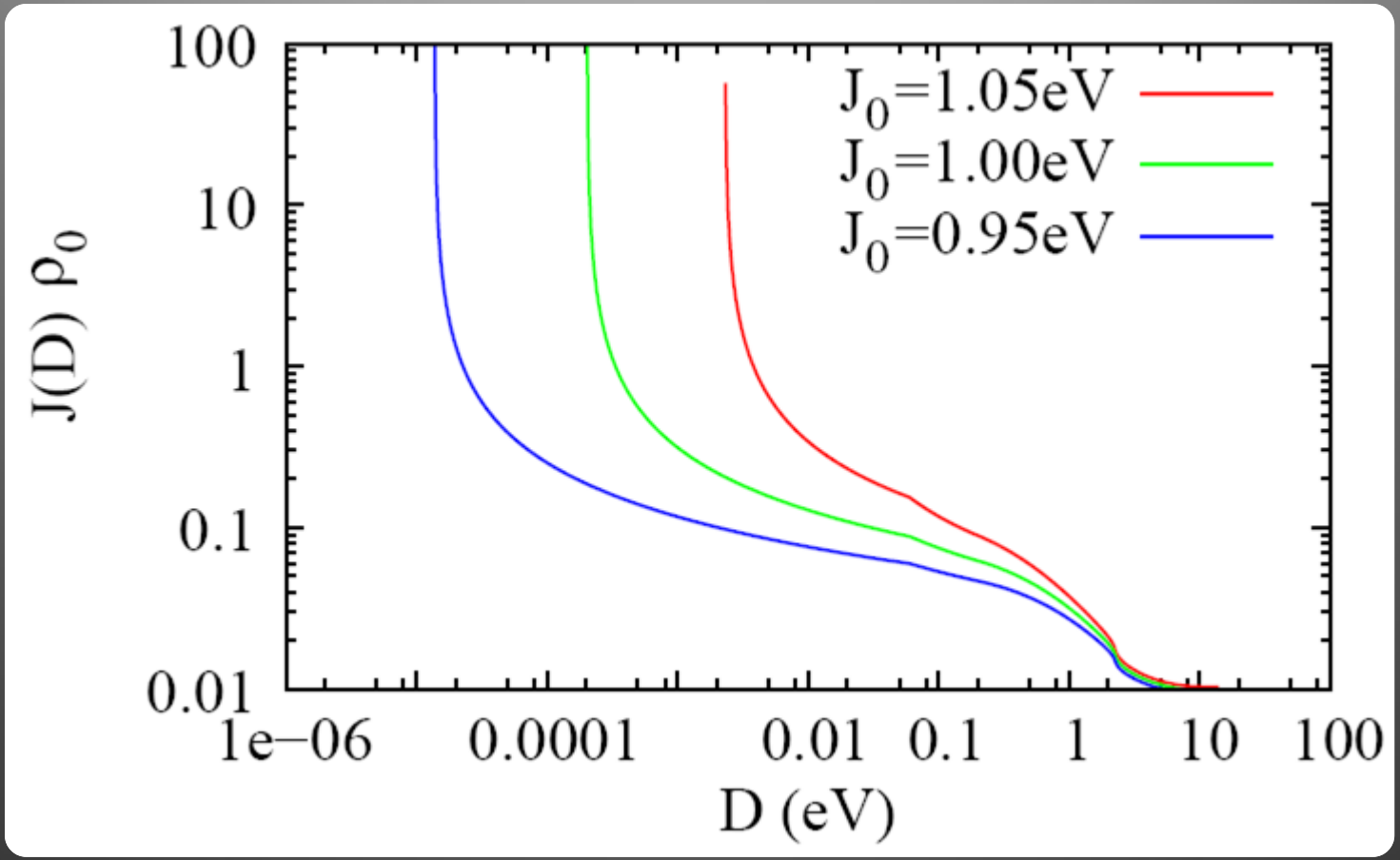

TW et al., PRB **81**, 115427 (2010)

- 10% change in bare coupling J_0 changes T_K by factor > 10
- Proximity to quantum critical point: $J_c \approx 1.1$eV

S=1/2 graphene Kondo models

Pseudogap Kondo problem

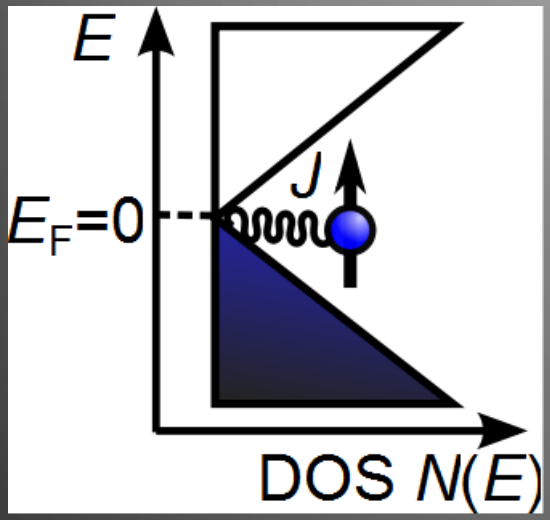

- $J < J_c$: Spin remains unscreened
- $J > J_c$: Spin screened despite zero DOS at Fermi level

C. R. Cassanello and E. Fradkin, PRB 53, 15079 (1996).
K. Ingersent, PRB 54, 11936 (1996).
A. Polkovnikov, S. Sachdev, and M. Vojta, PRL 86, 296 (2001).
M. Vojta and R. Bulla, PRB 65, 014511 2001.
L. Fritz and M. Vojta, PRB 70, 214427 2004.
A. V. Balatsky, I. Vekhter, and J.-X. Zhu, RMP 78, 373 2006.

Two channel Kondo problem

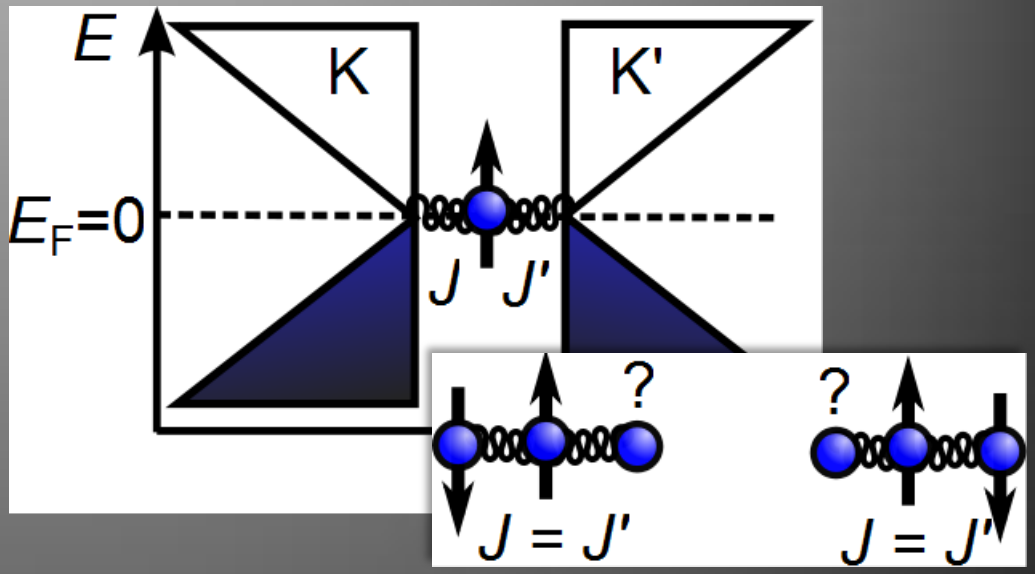

- Non Fermi liquid ground state

A. A. Abrikosov and A. A. Migdal, J. Low. Temp. Phys. 3, 519 (1970)
P. Nozieres and A. Baladin, J. Physique 41, 193 (1980).
A. C. Hewson's book + Refs. therein

K. Sengupta and G. Baskaran, PRB **77,** 045417 (2008).

Co adatoms on graphene: DFT calculations

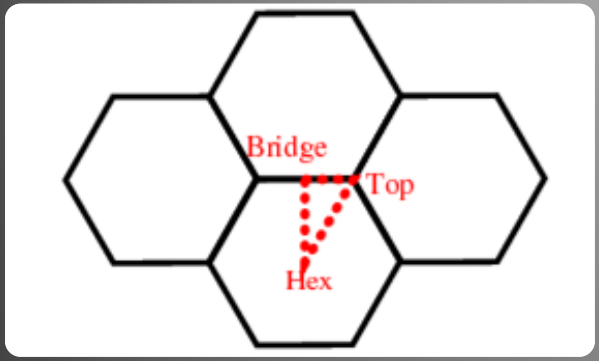

Energy relative to hex-site

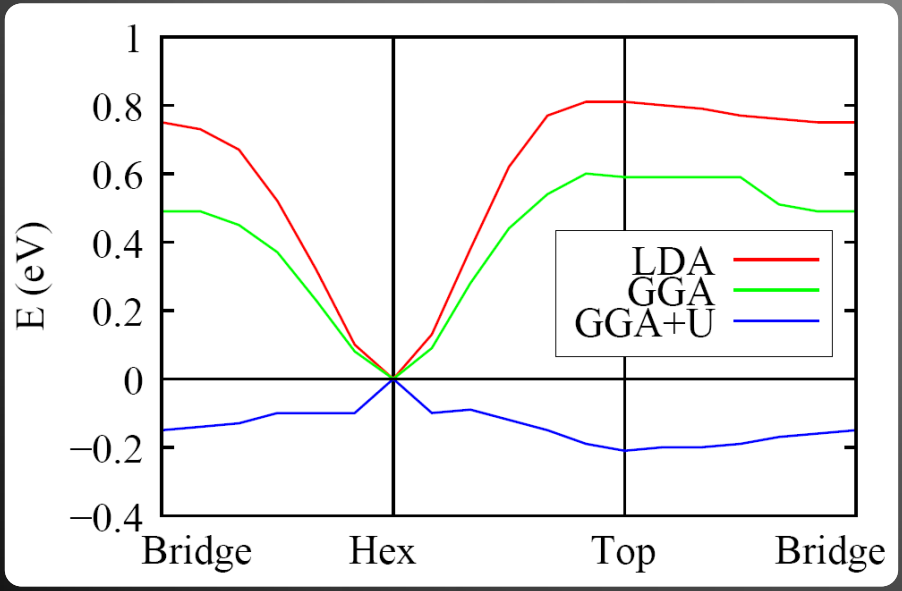

Magnetic moment of supercell

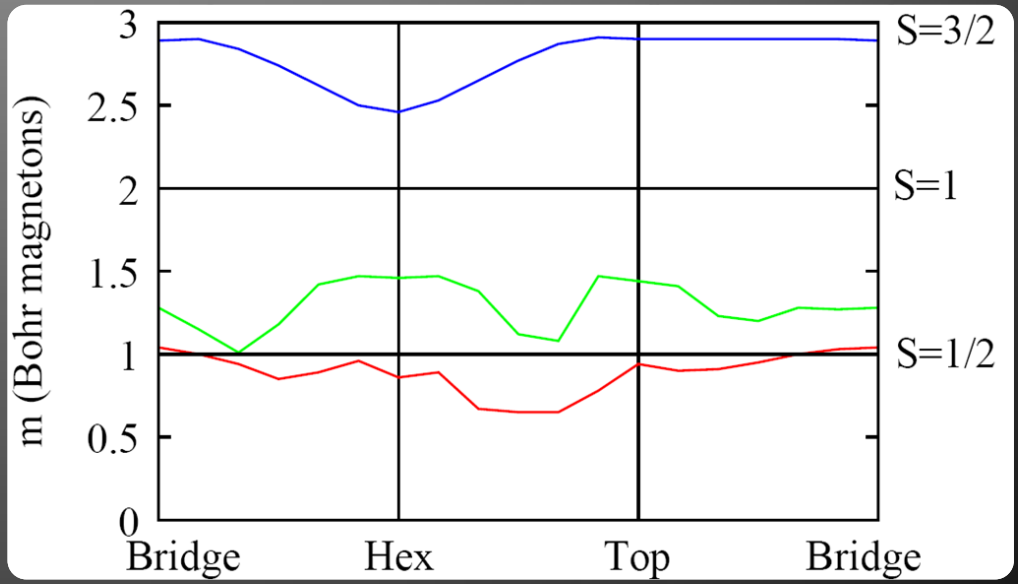

GGA+U: U=4eV, J=0.9eV

TW et al., PRB **84**, 235110 (2011)

Comparison of 3d adatoms on graphene

Magnetic moment (μ_B)	GGA			GGA+U		
	t	b	h	t	b	h
Cr	5.9	5.8	5.6	5.9	5.9	5.9
Mn	5.1	5.1	5.2	5.0	5.0	5.0
Fe	4.1	4.1	2.0	3.9	3.9	3.6
Co	1.1	1.1	1.1	2.9	2.9	2.6
Ni	0.0	0.0	0.0	0.0	0.0	0.0

Height above sheet (Å)	GGA			GGA+U		
	t	b	h	t	b	h
Cr	2.4	2.3	2.1	2.6	2.6	2.9
Mn	2.2	2.2	2.1	3.7	3.8	3.8
Fe	2.2	2.2	1.5	2.2	2.3	2.0
Co	1.9	1.8	1.5	2.2	2.2	1.8
Ni	1.9	1.8	1.6	1.8	1.8	1.5

Binding energy (eV)	GGA			GGA+U		
	t	b	h	t	b	h
Cr	0.49	0.50	0.47	0.34	0.34	0.33
Mn	0.35	0.34	0.42	0.30	0.28	0.28
Fe	0.24	0.22	0.71	0.29	0.25	0.27
Co	0.75	0.88	1.35	0.62	0.56	0.41
Ni	1.44	1.52	1.72	0.74	0.82	0.97

TABLE I. Magnetic moment of supercell, height above graphene sheet and energy relative h-site for 3*d* transition metal adator as obtained from GGA and GGA+U with $U = 4\,\text{eV}$ and $J = 0.9\,\text{eV}$. High-spin solutions are colored back, low-spin solutic red (grey).

TW et al., PRB **84**, 235110 (2011)

- **4s orbitals of adatoms remain localized**
- Local Coulomb interaction *U* affect inter-configuration energies ($E(s^1d^n)$-$E(s^0d^{n+1})$)
- Electronic configuration, adsorption geometry and migration barriers depend decisively on local Coulomb interactions

Graphene on transition metal surfaces

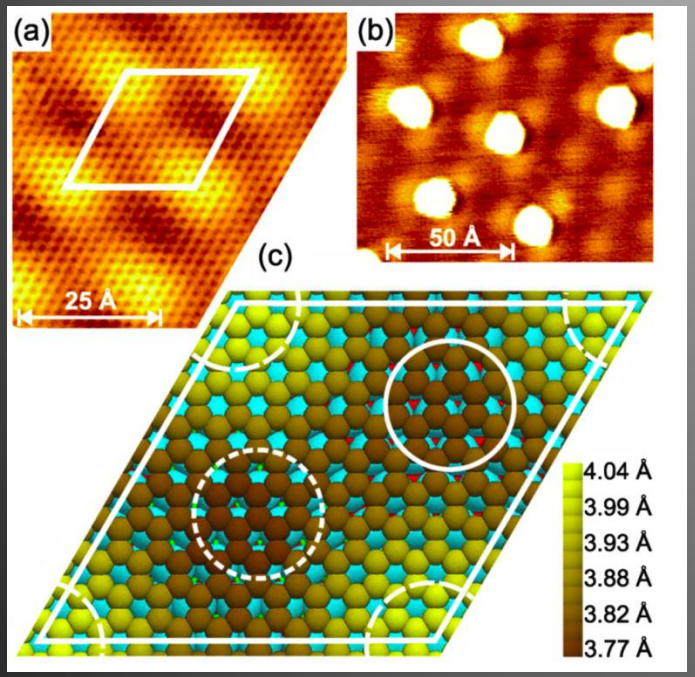

Upper panel: Graphene by CVD on Ir (111).
Alpha T. N'Diaye et al., PRL **97,** 215501 (2006).

Right panel: Hybrid structures of magnetic Eu and graphene on Ir(111).
D. F. Förster, TW et al., New J. Phys. (2012)

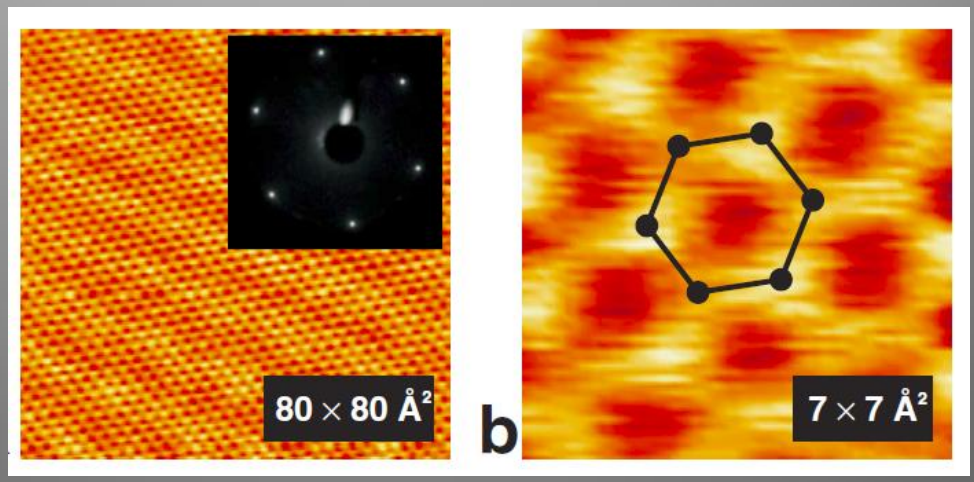

Graphene by CVD on Ni (111).

Y. S. Dedkov et al., PRL **100**, 107602 (2008)

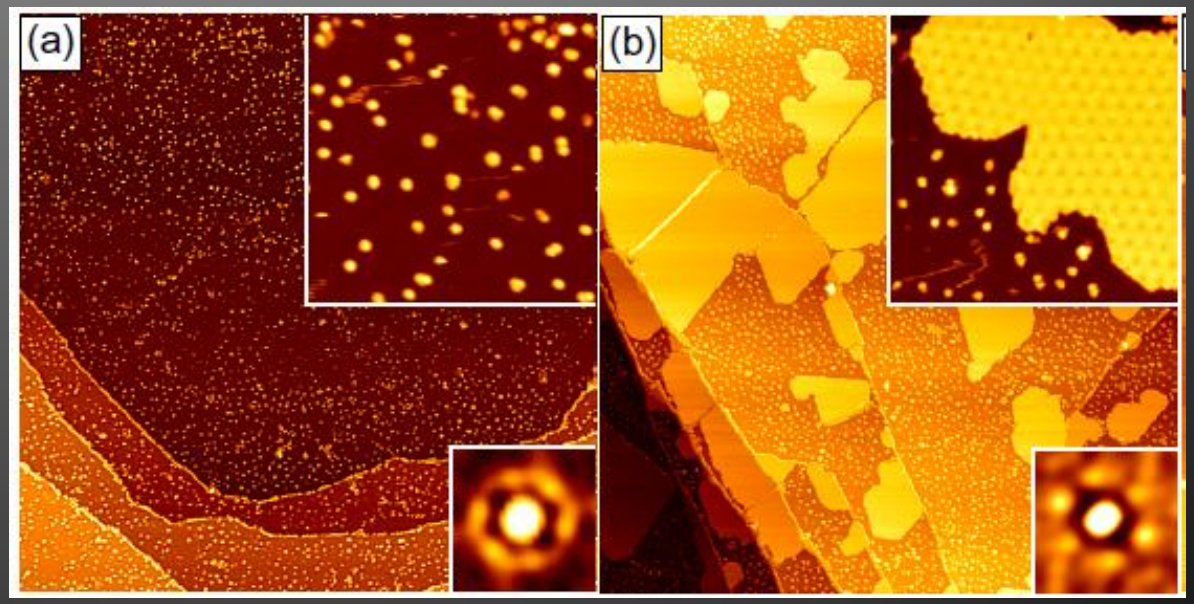

Band structures of graphene covered TM surfaces

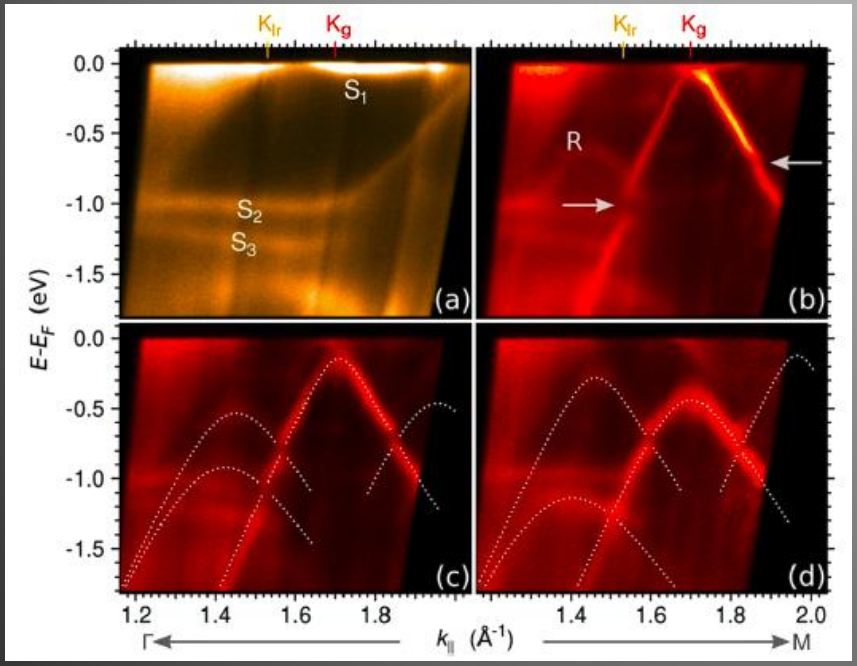

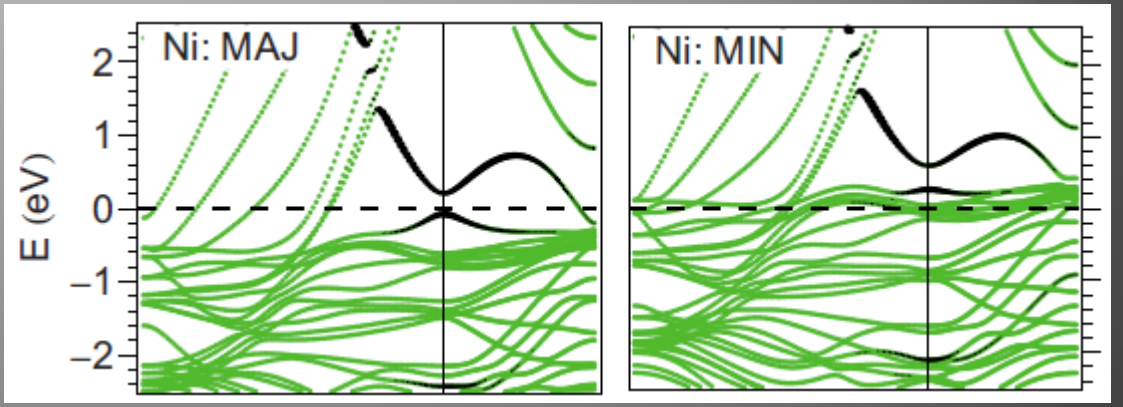

Right: Band structure of graphene on Ni (111).
P. A. Khomyakov et al., PRB 79, 195425 2009

Left: ARPES spectrum of graphene on Ir (111)
I. Pletikosic et al, PRL **102**, 056808 (2009)

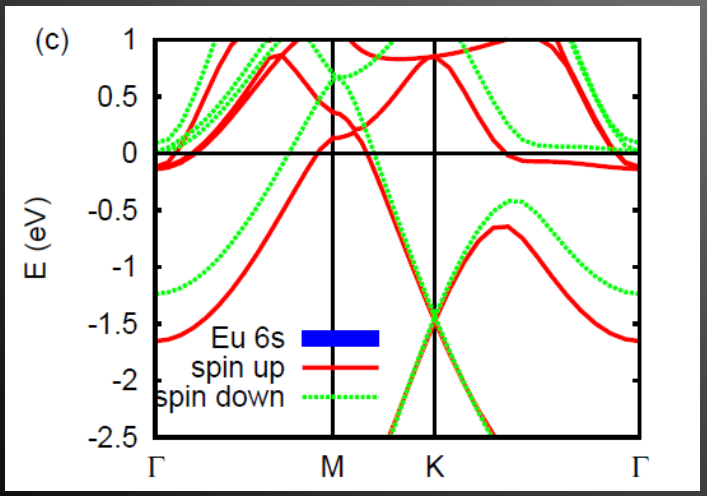

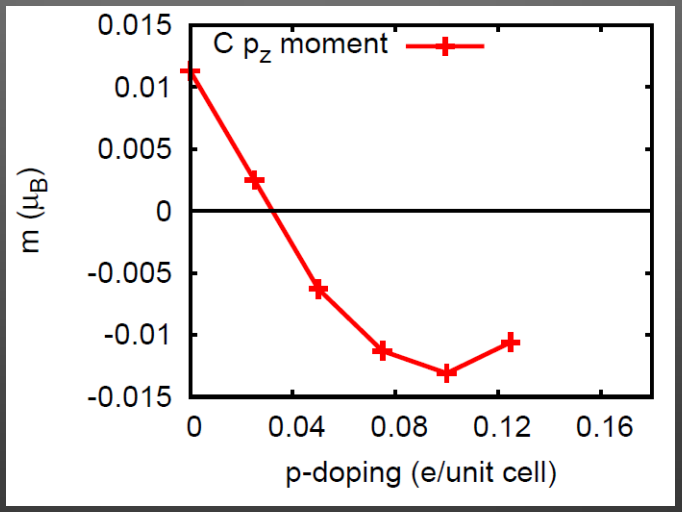

Left: Band structures of graphene with adsorbed p(2x2) Eu layers.

Right: Induced moments in graphene

“Invisibility” of graphene Dirac states to STM

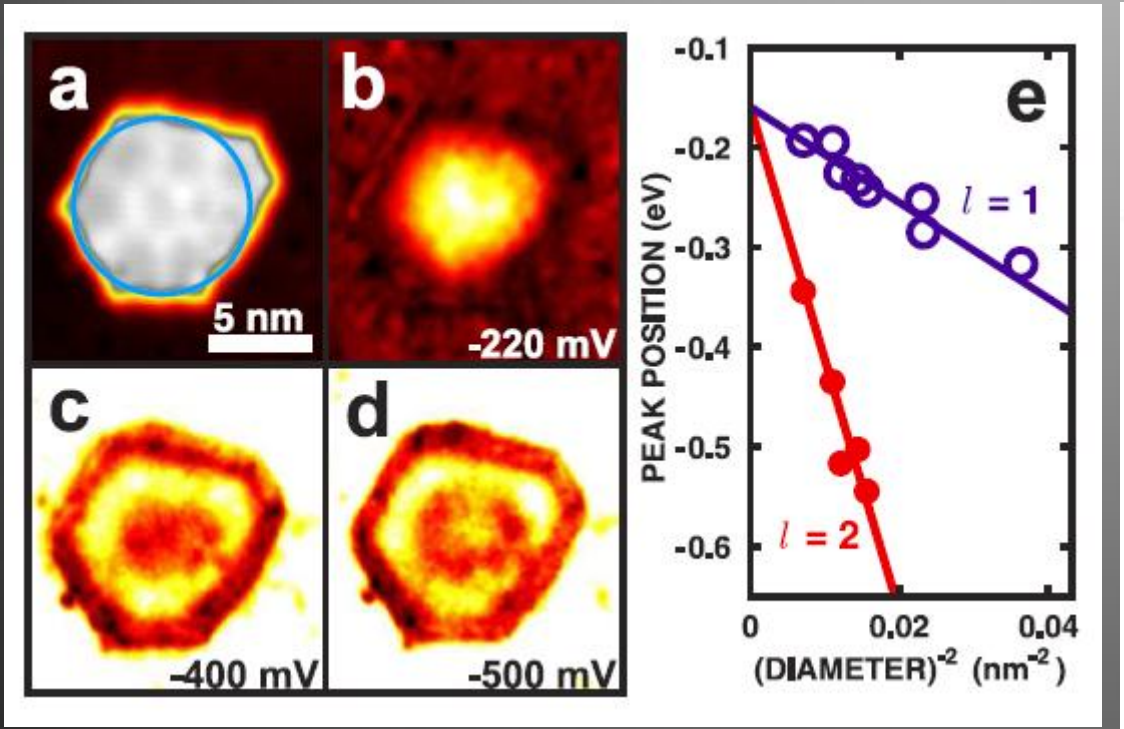

STM spectroscopy (dI/dU) maps of graphene islands on Ir (111).

S. Altenburg, TW et al., PRL accepted.
Similar results in PRL **108**, 046801 (2012).

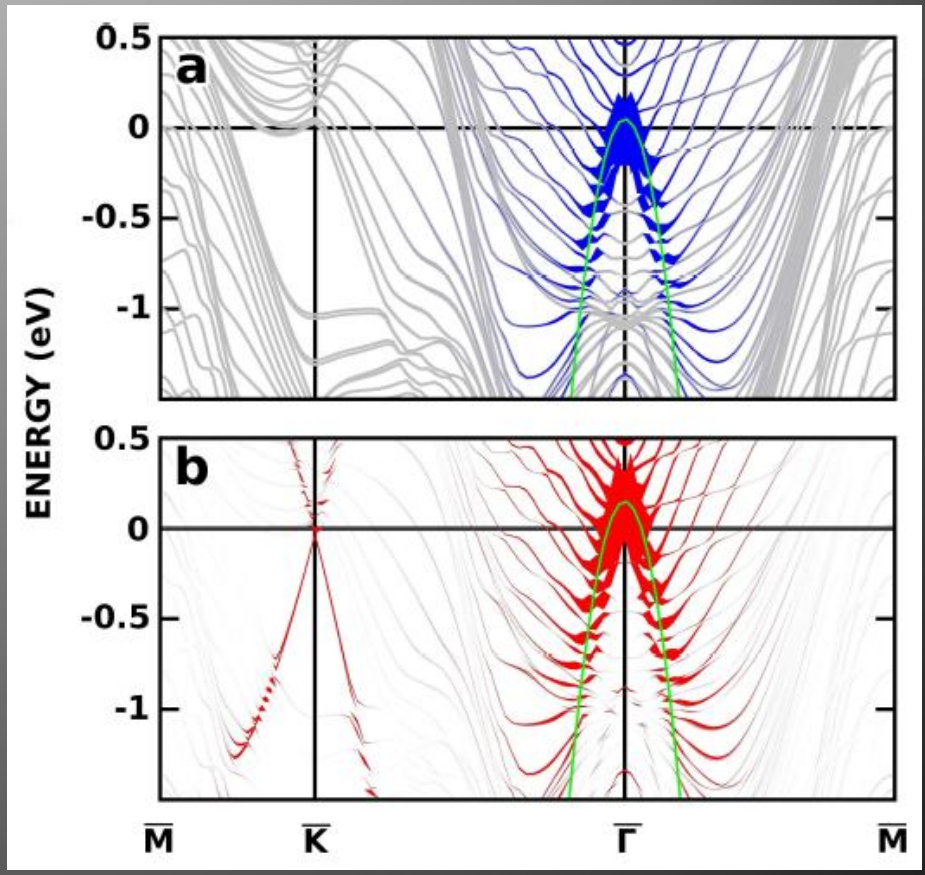

Band structure of Ir (111) (a) and graphene covered Ir (111) (b). Thinckess of lines = amplitude of wave functions at 5 Å above surface.

“Invisibility” of graphene Dirac states to STM

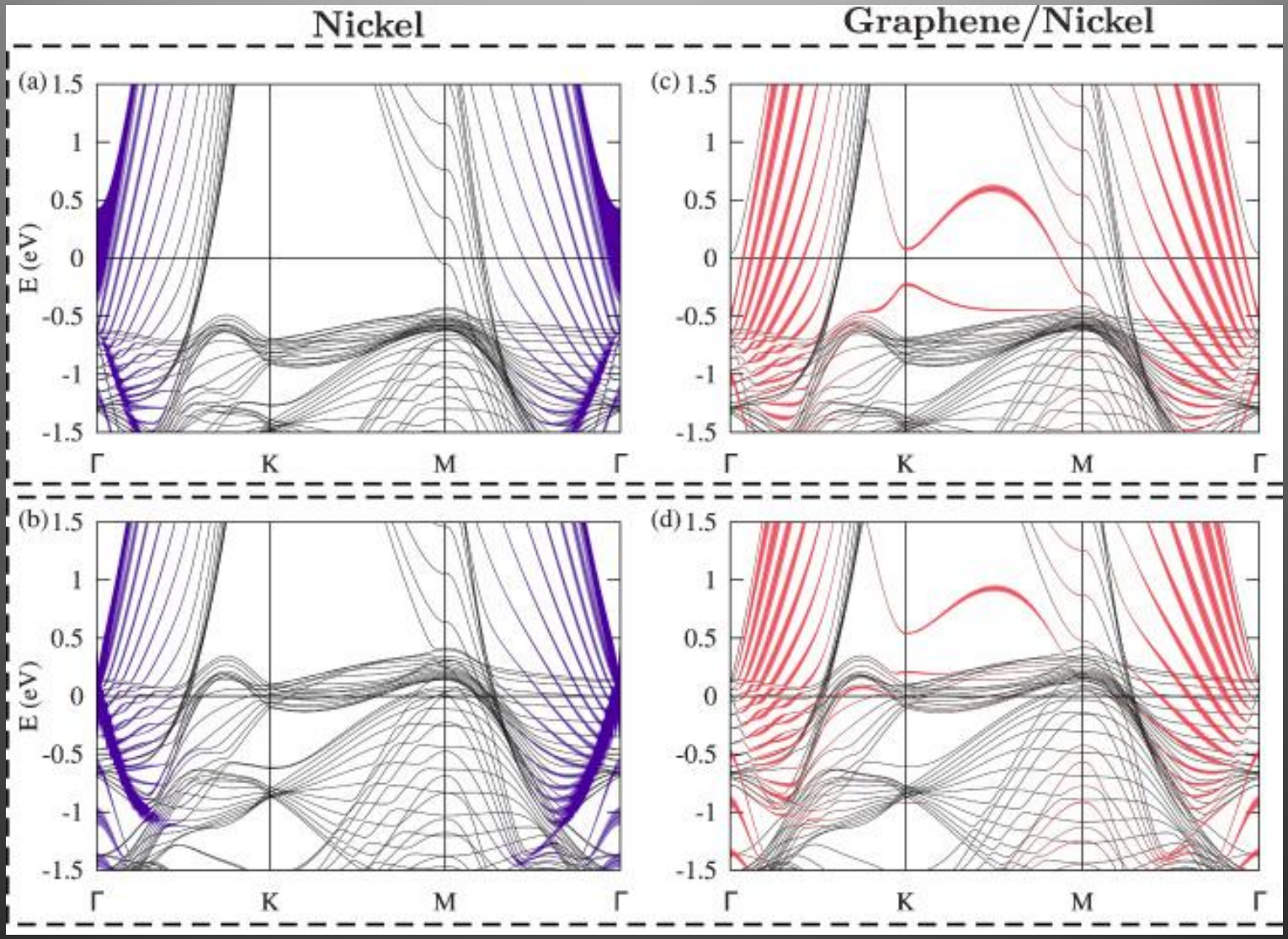

L. V. Dzemiantsova et al., PRB **84**, 205431 (2011)

Graphene on hBN substrates

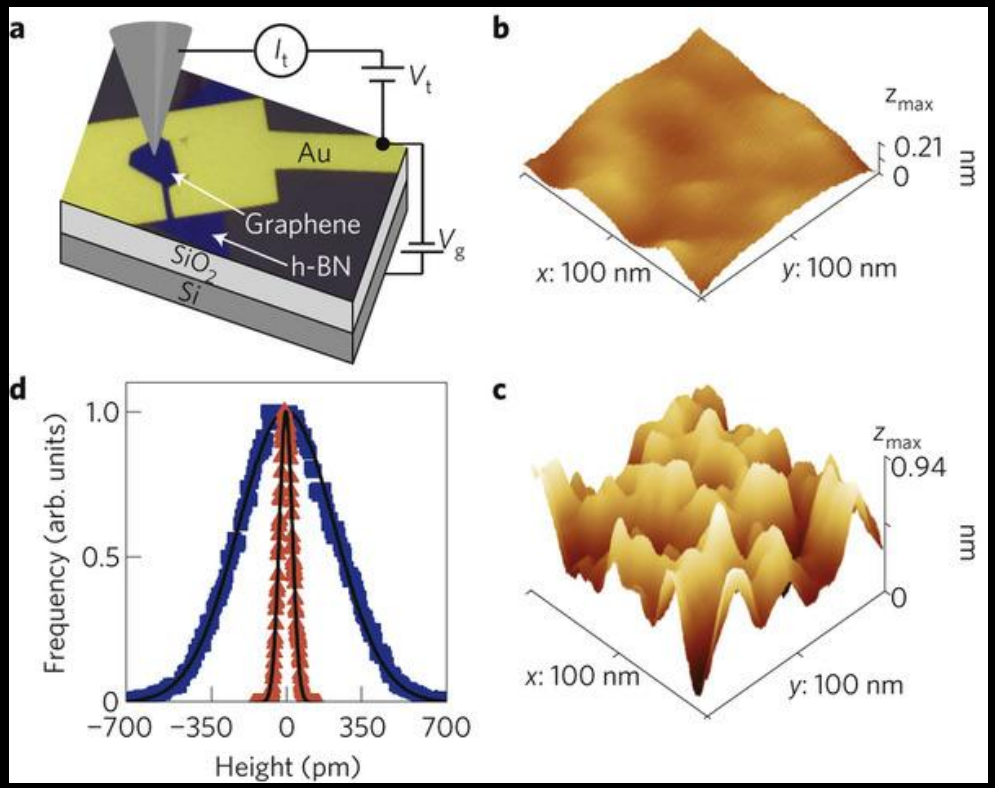

J. Xue et al , Nature Materials **10**, 282–285 (2011)

Vertical field effect transistors (arXiv:1112.4999)

Secondary Dirac points / minigaps (arXiv:1202.2870)

hBN substrates

- "Ultraflat" graphene
- Enhanced electron mobility
- Moiré structures

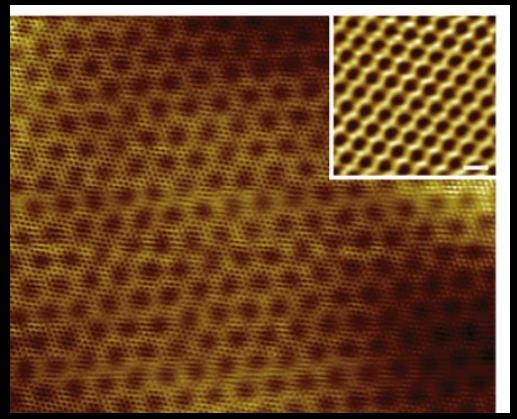

Ab-initio calculations of graphene on hBN

- Adhesion of graphene and h-BN through van der Waals forces
  - Simulation within LDA/GGA problematic:

    No long-range correlations taken into account
  - Alternative: ACFDT-RPA (Y. M. Niquet et al., PRA 68, 032507 (2003). J. Harl et al., PRB 81, 115126 (2010).)

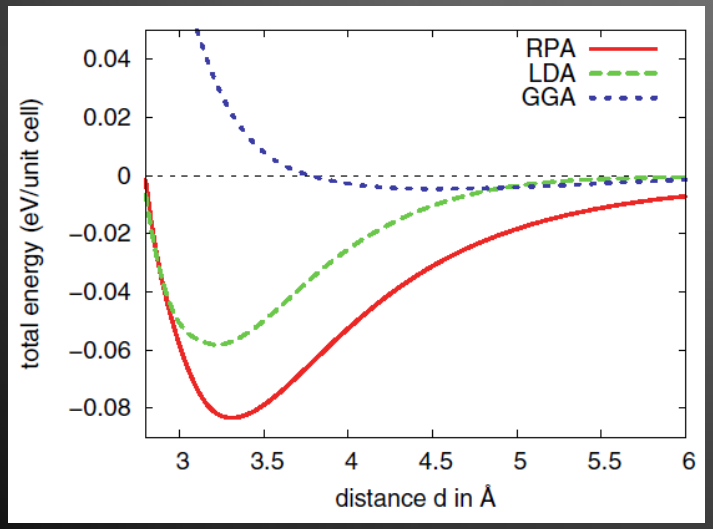

B. Sachs et al., PRB **84**, 195414 (2011)

- 2% lattice mismatch

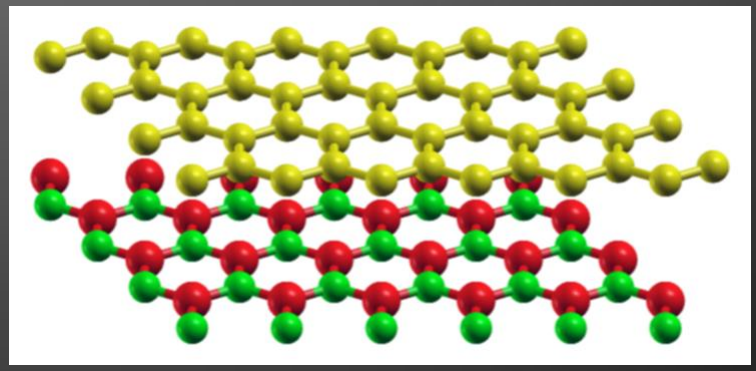

Structure of graphene on hBN: moiré?

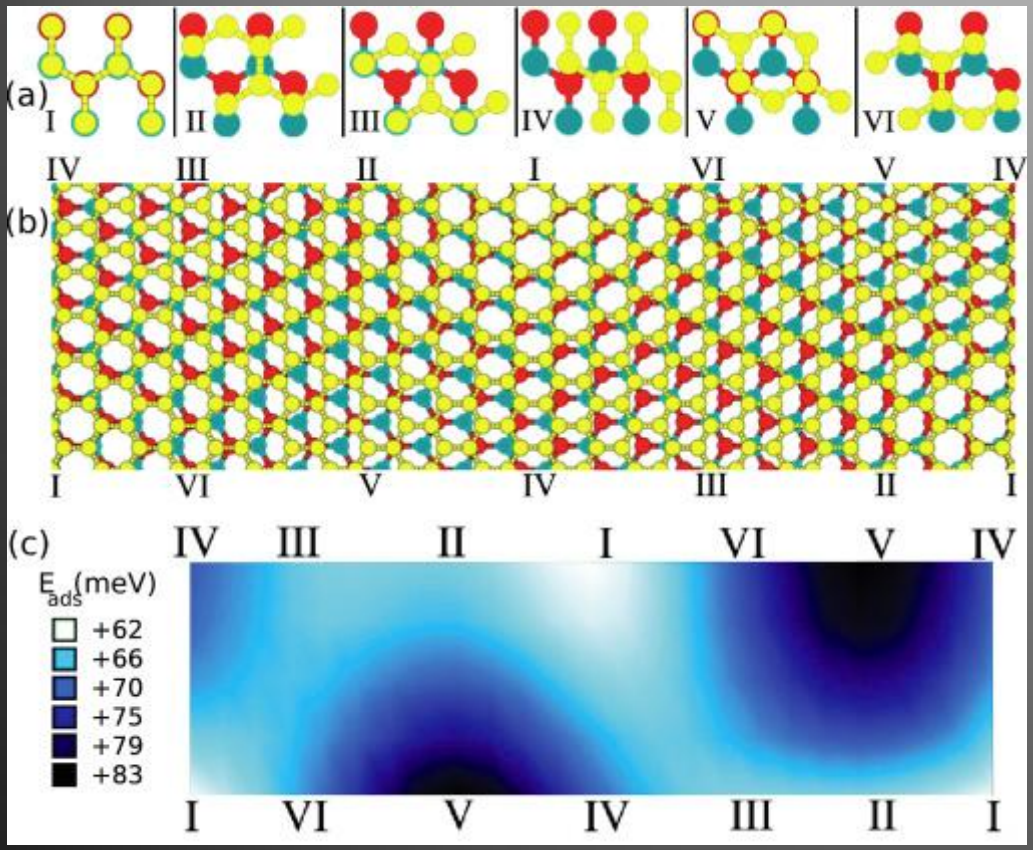

(a) Top view of the calculated stacking configurations for graphene on h-BN. (b) Moiré structure with persisting lattice mismatch. (c) Adhesion energy (E_{ads}) landscape in the moiré pattern (color coded).

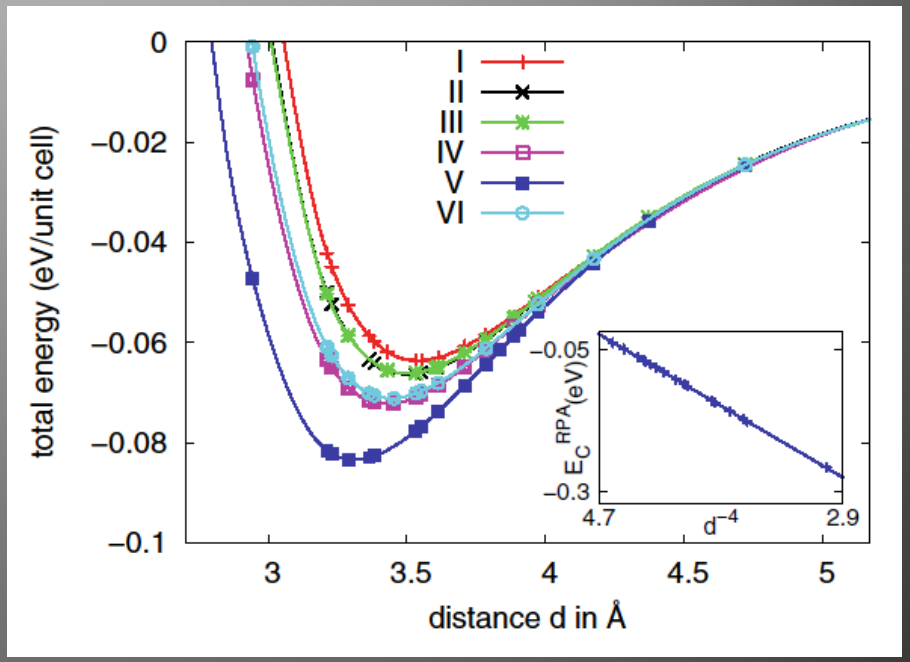

- Average adhesion energy loss upon Moiré formation: **14meV/2C-atoms**
- Energy to strain graphene to hBN-lattice constant: **40meV/2C-atoms**
- Strain energy for graphene and hBN at common optimized lattice constant: **18meV/2C-atoms**

B. Sachs et al., PRB **84**, 195414 (2011)

Effects of local sublattice symmetry breaking?

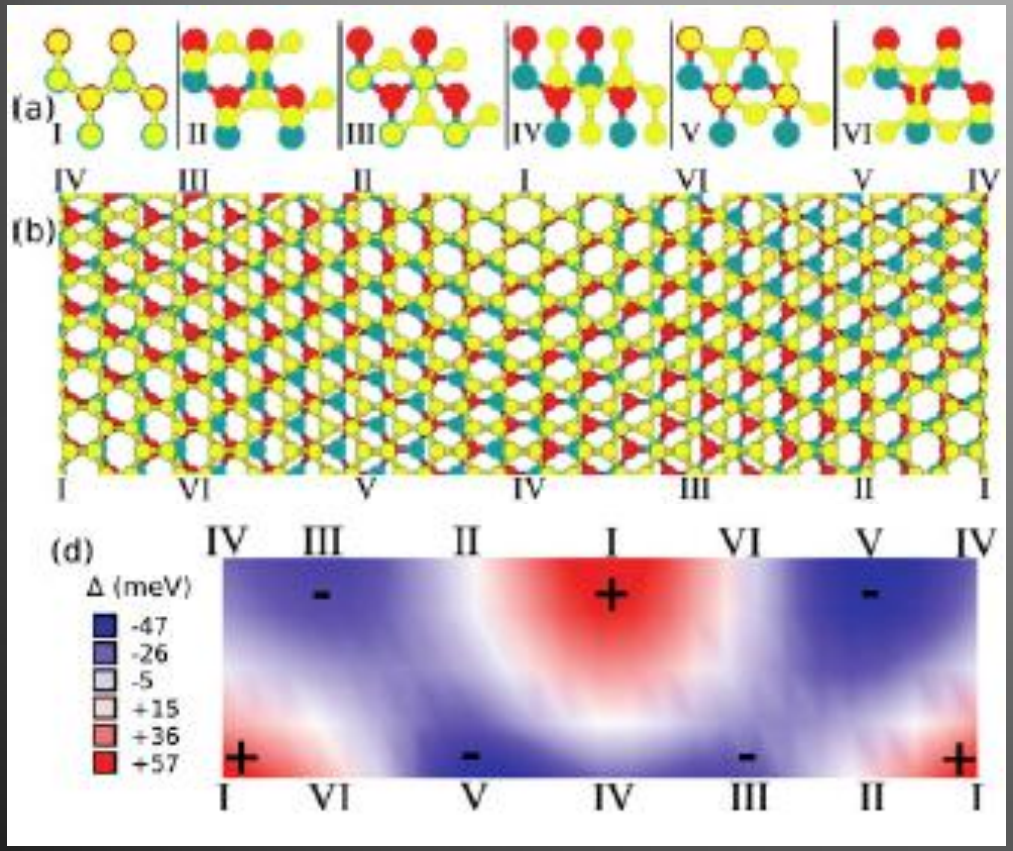

(d) Local sublattice symmetry breaking Δ

$$H = -t \sum_{\langle i,j \rangle} (a_i^\dagger b_j + \text{H.c.}) + \frac{1}{2} \sum_i \Delta_i (a_i^\dagger a_i - b_i^\dagger b_i)$$

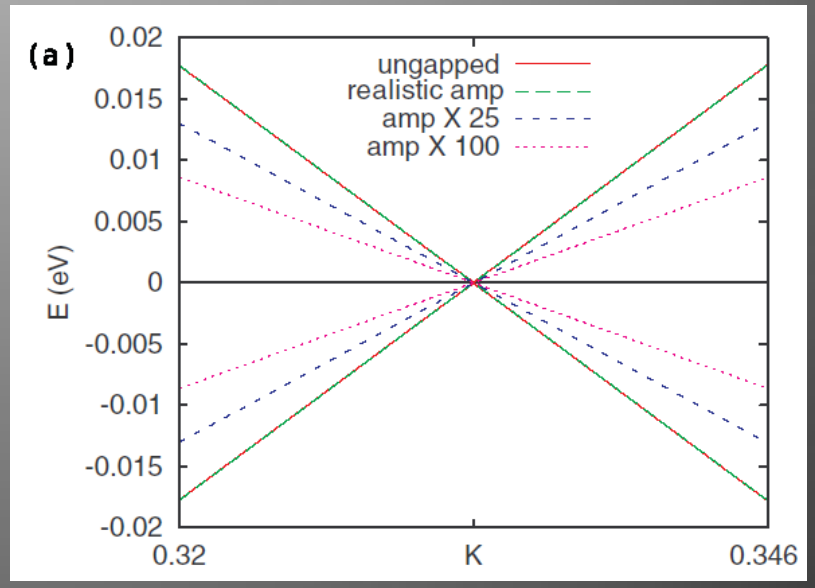

(a) Band structure of 20x20 moiré cell with sinusoidally modulated gap term

No gap opening if

$$1/N \sum_i \Delta_i = 0$$

B. Sachs et al., PRB **84**, 195414 (2011)

Real space signatures of modulated gap terms

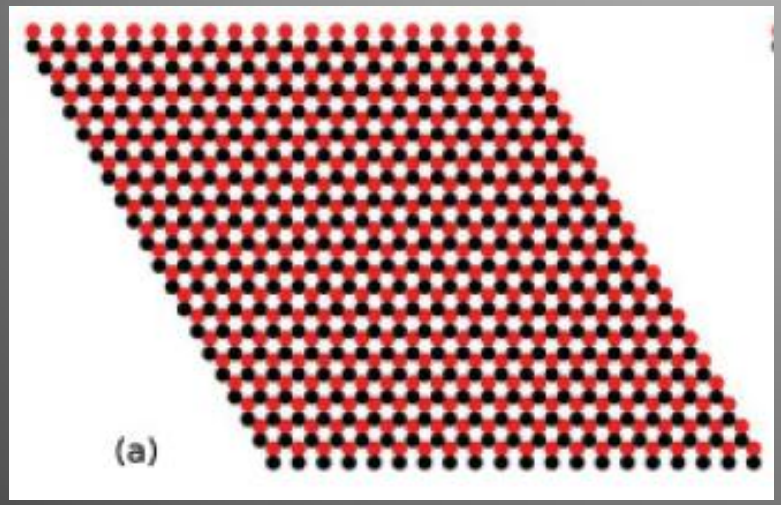

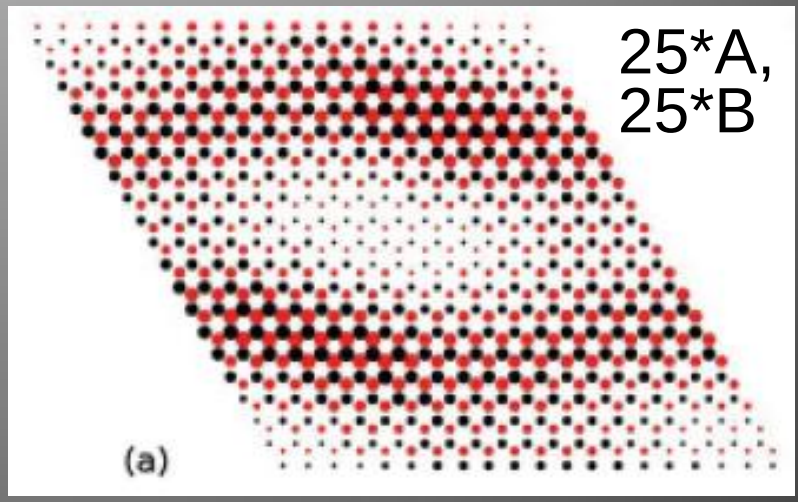

FIG. 6. (Color online) 20×20 graphene supercell (red/grey: sublattice A; black: sublattice B) with sinusoidally modulated gap terms with realistic amplitudes of $A = 18.6$ meV, $B = 42.0$ meV, and vanishing average gap ($\Delta_{\vec{G}=0} = 0$). The size of the dots depicts the contribution of each atom to states close to the Dirac point in an infinitesimal energy window around the valence-band maximum (a) and the conduction-band minimum (b).

B. Sachs et al., PRB **84**, 195414 (2011)

Grain boundaries in the hBN substrate

Topological states in single layer graphene

M. Zarenia, O. Leenaerts, B. Partoens, and F. M. Peeters
Department of Physics, University of Antwerp, Groenenborgerlaan 171, B-2020 Antwerpen, Belgium.

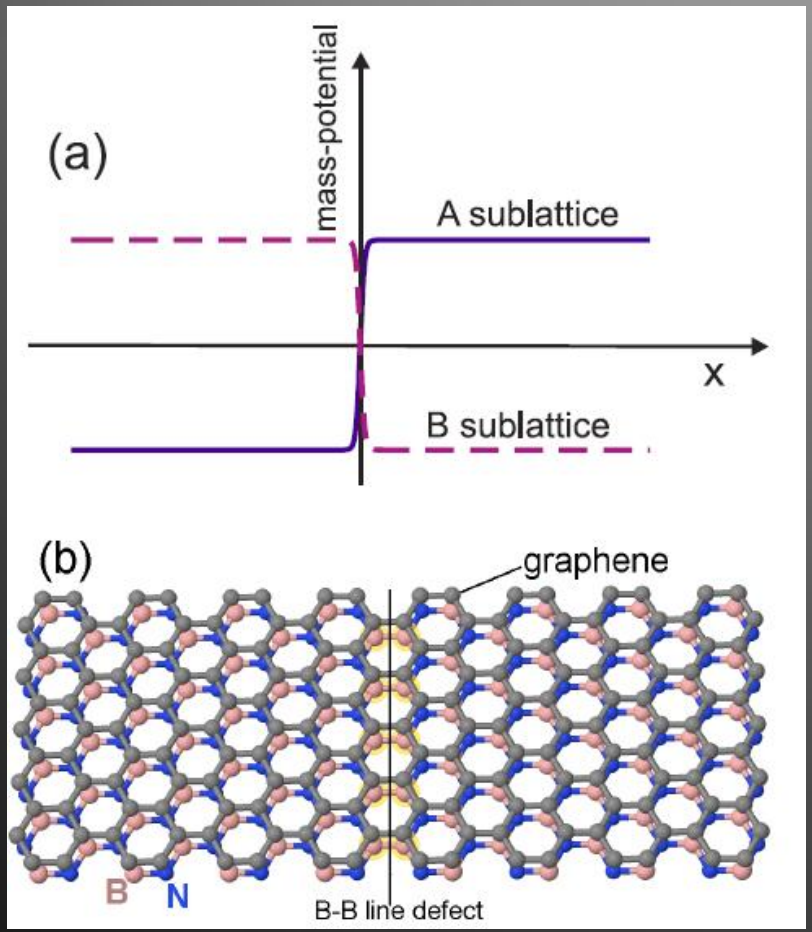

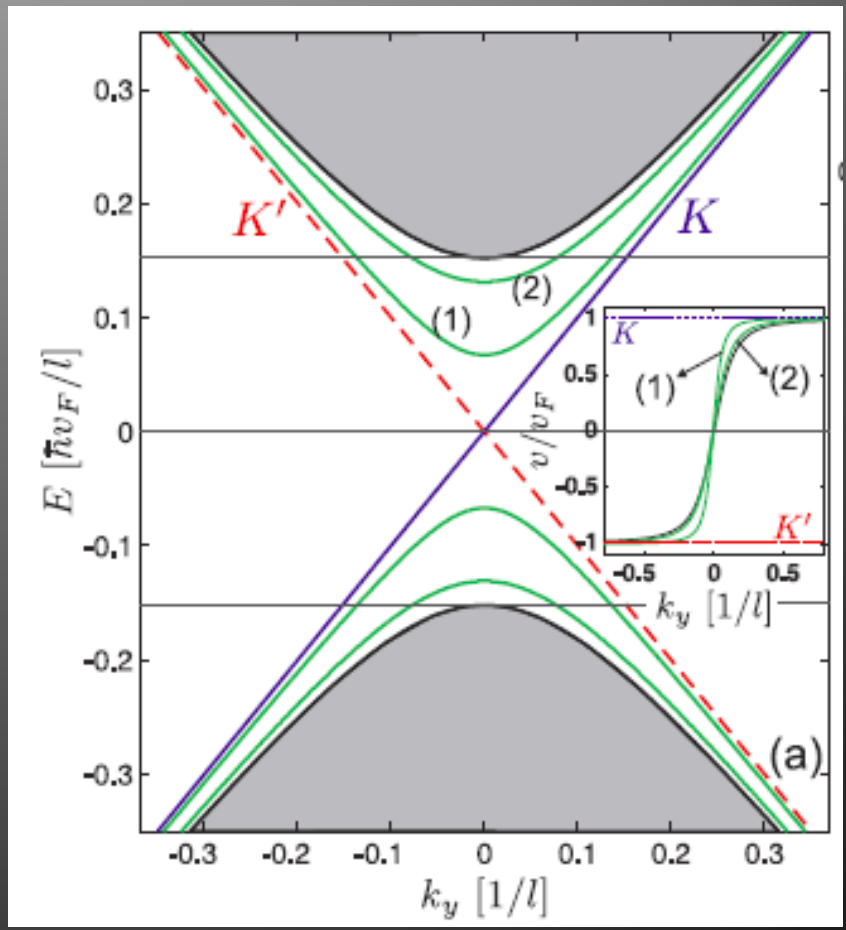

Summary

- Covalently bond adatom = TB vacancy ≠ real vacancy
- Orbitally controlled coupling of transition metal adatoms to graphene
- Metals-graphene hybrid materials
  - Doping tunable magnetism ?
  - Invisibility of graphene Dirac states to STM
- Graphene on hBN
  - Energetics of Moiré formation
  - Local sublattice symmetry breaking and “snake” states